The Influence of Compaction Methods on the Compressibility Characteristics of Cohesive Soils

Bashar Alibrahim

Submitted to the
Institute of Graduate Studies and Research
in partial fulfillment of the requirements for the degree of

Master of Science
in
Civil Engineering

Eastern Mediterranean University
January 2019
Gazimağusa, North Cyprus

Approval of the Institute of Graduate Studies and Research

Assoc. Prof. Dr. Ali Hakan Ulusoy
Acting Director

I certify that this thesis satisfies all the requirements as a thesis for the degree of Master of Science in Civil Engineering.

Assoc. Prof. Dr. Serhan Şensoy
Chair, Department of Civil Engineering

We certify that we have read this thesis and that in our opinion it is fully adequate in scope and quality as a thesis for the degree of Master of Science in Civil Engineering.

Asst. Prof. Dr. Eriş Uygar
Supervisor

Examining Committee

1. Prof. Dr. Zalihe Nalbantoğlu Sezai

2. Assoc. Prof. Dr. Huriye Bilsel

3. Asst. Prof. Dr. Eriş Uygar

ABSTRACT

Over the past decades, engineers aimed to enhance the engineering properties of natural soil deposits, by compaction to reduce compressibility, permeability and increase bearing capacity. The most common compaction methods used in the laboratory are the Standard Proctor compaction in which, dynamic compaction is performed to obtain compaction characteristics of soils. However, insitu application of most common shallow compaction methods involve the static compaction which is implemented with the use of compaction rollers. The aim of this study is to investigate the influence of compaction method (dynamically and statically) on the engineering properties of selected soils. In order to meet this objective, an extensive laboratory test program is conducted on two selected soils that have significant variation among their plasticities and composition. Various dynamic compaction efforts are conducted at different moisture contents, which are also simulated using static compression. The compacted specimens are tested for measurement of Electrical Resistivity, Undrained Shear Strength and Compressibility characteristics. Results indicate that static compaction reduces the electrical resistivity, and the undrained shear strength. On the other hand, the compressibility and the swelling potential of the compacted specimens are observed to increase when the static compaction is used. The outcomes of this research indicate that field sampling and testing is required for effective design and control of engineering properties of compacted fills, as the method of compaction is observed to have a significant impact on the engineering behavior of soils.

Keywords: Static compaction, Dynamic compaction, Compaction efforts, Electrical resistivity, Undrained shear strength, Compressibility

ÖZ

Son yıllarda mühendisler toprak dolguların zemin emniyet gerilmesini arttırmak amacıyla, toprak yoğunluğunu artırarak geçirimliliği ve sıkışabilirliği azaltmayı hedeflemiştir. Başlıca kompaksiyon (sıkıştırma) yöntemleri, genellikle laboratuarda yürütülen Standart Proctor (dinamik sıkıştırma) testi ve çoğunlukla sahada gerçekleştirilen statik kompaksiyondur. Bu çalışmanın amacı, iki tip kohezyonlu toprak üzerinde farklı iki kompaksiyon yönteminin (dinamik ve statik) etkisini araştırmaktır. Bu amacı gerçekleştirmek için, plastisite indeksleri ve içerikleri arasında önemli farklılıklar bulunan iki tip seçilmiş toprak üzerinde kapsamlı laboratuar deneyleri yapıldı. Çeşitli su muhtevalarında statik ve dinamik kompaksiyon sonuçları karşılaştırılmıştır. Elde edilen numunler üzerinde Elektrik iletkenliği, Drenajsız kayma dayanımını deneyleri uygulanmıştır. Sonuçlar statik kompaksiyon yönteminin, elektrik iletkenliği özelliğini ve drenajsız kayma dayanımını düşürdüğü gözlemlenmiştir. Diğer taraftan şişme ve konsolidasyon özelliklerinin de arttığı gözlemlenmiştir. Bu araştırmanın sonuçları kompaksiyon uygulanan zeminlerin mühendislik özelliklerinin kullanılan yöntemden etkilendiğini ve dolayısı ile araziden numune alımı ve deney yapılmasının gerekliliğini göstermiştir.

Anahtar kelimeler: Statik kompaksiyon, Dinamik kompaksiyon, Kompaksiyon enerjisi, Elektriksel iletkenlik, Drenajsız kayma dayanımı, Konsolidasyon

Dedicated to the memory of my mother, Suhaila

ACKNOWLEDGMENT

I would like to thank my supervisor Asst. Prof. Dr. Eriş Uygar for his delightful guidance and patience throughout the progress of developing my thesis, and not to mention the endless time that he spent with me, regardless of the heavy duties that he has.

I would also like to thank every single member of the Civil Engineering Department at Eastern Mediterranean University for their assistance, encouragement and for enabling me to use the laboratory facilities in the Soil Mechanics Laboratory.

Finally, I would like to thank my family for their endless supports.

My kindest regards for all of you.

TABLE OF CONTENTS

LIST OF TABLES

LIST OF FIGURES

LIST OF SYMBOLS AND ABBREVIATIONS

A	Cross-Sectional Area of the Compacted Specimen (cm^2)
a,b,c,and d	Polynomial Coefficients in the Dynamic Compaction Analysis Method
ASTM	American Society for Testing and Materials
CBR	California Bearing Ratio
CEC	Cation Exchange Capacity
Cc	Compression Index
CH	Inorganic Clay of High Plasticity
Cr	Rebound Index
d_p	Distance Between Electrodes (cm)
e	Void Ratio of the Specimen
e(σ')	Void Ratio at Given Effective Stress
e_0	Initial Void Ratio
ER	Electrical Resistivity (ohm-cm)
g	Gravitational Acceleration (m/s^2)
Gs	Specific Gravity of the Soil
h_d	Drop Height of the Hammer (m)
H_m	Mold Full Height (cm)
I	Current (A).
Ke	Kinetic Energy (J)
LL	Liquid Limit
L_p	Length of Penetration (cm)

m_h	Mass of the Compaction Hammer (kg)
m_s	Dry Mass of the Specimen (g)
m_t	Bulk Mass of the Specimen (g)
m_w	Mass of Water Within the Specimen (g)
m_{ws}	Mass of Wet Soil (g)
n	Porosity of the Specimen
PI	Plasticity Index
PL	Plastic Limit
Sr	Degree of Saturation
V	Total Volume of the Specimen (cm^3)
V_d	Voltage Drop Measured at Resistor (Volt)
v_{im}	Velocity of The Hammer Just Before the Impact in Dynamic Compaction Test (m/s)
V_s	Volume of Solids Within the Specimen (cm^3)
V_v	Volume of Voids Within the Specimen (cm^3)
V_w	Volume of Water Within the Specimen (cm^3)
w_c	Water Content
w_{opt}	Optimum Moisture Content
α and β	Fitting Parameters in the Preconsolidation Estimation Method
ρ_{bulk}	Bulk Density (g/cm^3)
ρ_d	Dry Density (g/cm^3)
ρ_{max}	Maximum Dry Density (g/cm^3)
ρ_w	Density of Water at 23℃ (0.997 g/cm^3)
σ'	Applied Effective Stress (kPa)

Ω	Resistor Capacity (Ohm)

Chapter 1

INTRODUCTION

1.1 General

Engineered fills such as highway embankments and land fill liners are compacted for improvement of their compressibility, shear strength, hydraulic conductivity etc. The improvement by compaction is achieved by reducing the volume of air within a soil medium by packing the soil particles into a more interlocked fabric. Hence, in essence compaction is the process of increasing the density of soil and reducing the magnitude of the voids. There are various compaction methods available to be applied depending on the soil type and the depth of improvement required. The most commonly used method for shallow improvement of fills is called the static compaction method with or without vibratory action. However, it is interesting that the method used in the laboratory for design of such a field application utility relies on the dynamic compaction methods conducted in the laboratory.

1.2 Problem Statement

The parameters that affect the engineering properties of compacted soil medium are well documented within the literature. However, the influence of the compaction methods on the engineering characteristics of soil is scarce in the literature. For instance, only few of the conducted research investigated the comparison of the influence of static and dynamic compaction on the engineering characteristics [1]. The influence of compaction methods on the electrical resistivity, undrained shear strength and compressibility are not thoroughly investigated. This is extremely vital, since the

engineering characteristics are determined in laboratory using remolded specimens prepared by dynamic compaction but the field compaction applied on site is mostly by static compaction. This study investigates whether the compacted soil using the static method poses similar engineering properties to the dynamically compacted soil or the results from specimens prepared with these methods diverge significantly.

1.3 Objective

This study focuses on the influence of two compaction methods, static and dynamic on the electrical resistivity, undrained shear strength, and compressibility. For this purpose, dynamic compaction effort is simulated using static pressure. This study also provides insight into how these compaction methods influence the soil behavior.

1.4 Research Methodology

In order to investigate the influence of compaction methods on the engineering properties of remolded specimens, two types of soils with significant differences among their plasticities, and particle size distribution are selected. Both dynamic and static compaction methods are considered at various compaction efforts. In addition, the influence of moisture content on the compaction performance and engineering characteristics are reviewed. One specimen from every compaction is obtained in order to test the electrical resistivity and the undrained shear strength of the specimen. In addition, the compressibility tests are conducted for the specimens at the optimum water content for each compaction effort applied.

1.5 Dissertation Content

This dissertation is basically composed of five main chapters. In this chapter a brief background information on the soil compaction and discussion of the objective of this study are presented.

Chapter 2, discusses and examines the previous studies within the literature such as; soil origin, compaction methods, the effect of compaction on the engineering properties, the electrical resistivity and the compressibility of soils.

Chapter 3 presents the experimental soil location and its properties. Provides step by step guidelines that includes: the adopted testing methods and analysis procedures.

Chapter 4 contains the obtained testing results altogether with comprehensive explanations and discussions of the observed behaviors. The dissertation is concluded in chapter 5, which contains a summary of the finding and suggestions for future studies.

Chapter 2

LITERATURE REVIEW

2.1 Introduction

The effect of density and the water content on the behavior of compacted soil is extensively presented in the literature [2,3,4]. However, the effect of the compaction methods on the engineering properties of the compacted specimen is scarce. In this chapter, a summary of the published research about the influence of compaction methods on the engineering behavior of compacted soil is presented, considering electrical resistivity, undrained shear strength and compressibility parameters of soils.

2.2 Soil Origin

Soils are formed through the process of rock weathering [2]. Physical and chemical weathering processes disintegrate the parent rock into a smaller fragment that varies in size and surface roughness [3]. Chemical weathering processes morph the crystal and the chemical composition of the parent material causing changes in physical and chemical properties of soils [4]. In addition; the weathering process, the soil particles may undergo transportation by means of various physical actions such as; gravity, flow of water, sedimentation, glaciation, wind ...etc. The soils deposited under the acts of flowing water are called alluvial soils. On the other hand, a soil which remains in the same place after it is derived from the parent material is called a residual soil [2,3,4]. In this research, an alluvial soil and a residual soil deposit from Famagusta are selected.

2.2.1 Alluvial Soil

When the weathered fragments of parent material are deposited by means of flowing water, this type of deposition is called alluvial soil. The transported fragments may range between gravel and clay sized particles. However, the deposited soil pockets are rather uniform as shown in Figure 1. On the other hand, void ratio and the bulk density of these deposits vary along the depth and horizontal distances exhibiting an irregular behavior in terms of shear strength and compressibility [2,4].

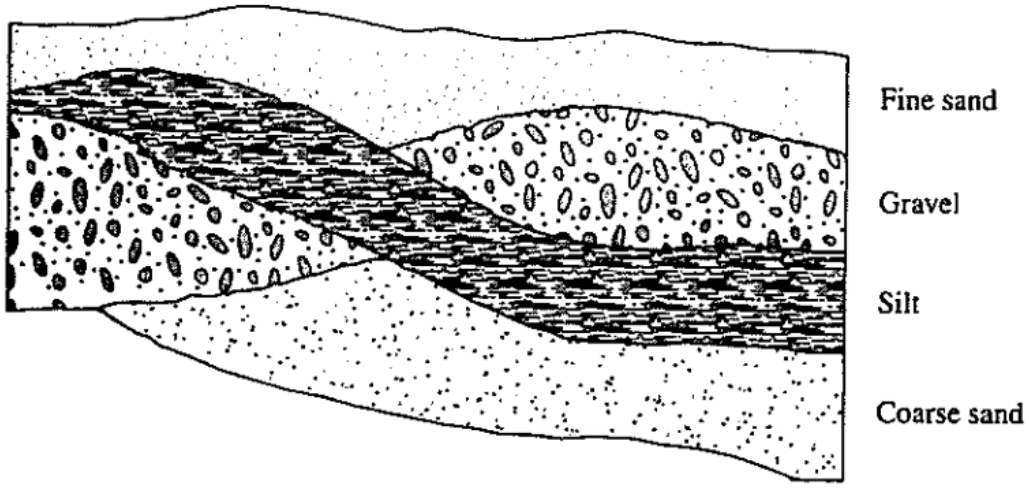

Figure 2.1: Schematical presentation of the alluvial deposits [2].

2.2.2 Residual Soil

When the weathered fragments of the parent material are not transported by any means, this type of formation is called residual soil. Residual soils are highly common in places where temperature and humidity motivate the chemical weathering processes resulting in a relatively fast weathering rate. Hence, the fragments accumulate faster than the transportation rate, such soils may have a wider range of particle size distribution and rich in oxides especially hematite [2,3,4].

2.3 Compaction

Compaction is the process of increasing the dry density of a given soil medium by reducing the volume of air voids for engineering purposes. The degree of compaction is mainly influenced by the water content and the compaction effort. In most cases, higher compaction effort results in an enhancement of the shear strength and the compressibility of the soil medium [3]. There are various methods of compaction used in practice for soil stabilization and to produce engineering fills such as highway embedments and impervious landfill liners. In laboratory, most common methods for testing compaction characteristics of cohesive soil are; dynamic compaction and static compaction [2].

2.3.1 Dynamic Compaction

Compaction characteristics of a fine-grained soils are commonly determined in laboratory using dynamic compaction such as; standard Proctor compaction or the modified AASHTO test, both of which have similar test procedures and mechanisms. These tests are performed by the application of an impact force on the soil surface multiple times till the required effort is achieved. The impact force is produced by a steel rammer which is dropped from specific height on the soil surface [3]. Various dynamic compaction efforts can be generated by changing the rammer mass, the drop height of the rammer, the number of layers and the number of blows applied to each layer surface. The compaction effort has a direct impact on the relevant optimum water content and the achieved dry density, such that; as the dynamic compaction effort increases, the optimum water content is reduced and the maximum dry density is increased [1,3].

2.3.2 Static Compaction

Static compaction is referred to the process of compacting the soil using constant rate of compression. The relation between the required stress to achieve a specified target bulk density reduces as the water content increases. This implies that static compaction requires less energy compared with standard Proctor compaction, especially when the molding water content is increased above the optimum water content [5].

The compaction characteristics of a given soil can be obtained using static compaction method as long as the rate of the compaction is slow enough to allow excess pore water pressure to dissipate or expelled out of the soil medium [1]. As the static compaction exhibits a parabolic relation between the dry density and the water content, an equivalent static stress can be predicted to represent the results of the dynamic compaction. Table 2.1 presents the equivalent static stresses suggested by various researchers for the Standard Proctor compaction effort at optimum water content.

Table 2.1: The suggested equivalent static stresses for the standard Proctor compaction at optimum water content.

Author	Equivalent Static Stresses (kPa)
Hogentogler, 1937. [6]	896
Reddy and **Jagadish, 1995. [5]**	4330
Sharma, Sridharan, and Talukdar, 2016. [7]	820

As shown in Table 2.1 there is a significant variation in the stresses obtained. This can be linked to the variations of the test setups and the soils used [1]. The size of the static compaction mold and the rate of compression, soil gradation and plasticity as well as

the optimum moisture content can be considered as the most important factors affecting the equivalent static stress. However, it can be stated that the equivalent static stress obtained by Reddy and Jagadish [5] is significantly higher compared to others given in Table 2.1. It can be speculated that this may be due to presence of high contact (friction) between the compaction mold and the compaction rod used in that study. In addition, in their study the mode of compaction was carried out in the opposite direction compared to the others and also more importantly the rate of compression was approximately 0.25MPa/s, which is significantly higher.

2.4 Effect of Plasticity Properties on the Compaction Characteristics

The process of obtaining the compaction characteristics parameters is quiet time and effort consuming, regardless of its simplicity. Thus, predicting these parameters using index properties such as the liquid limit and the plastic limit is quite beneficial [8]. Pandian et al. (1997) in their study on the effect of Liquid limit on the compaction characteristics found that there is an increasing linear relationship between the water content of the compacted specimen and the liquid limit. However, this relation is also dependent on the degree of saturation for the specimen. Based on these observations they were able to develop a mathematical model that can predict the compaction curve based on liquid limit and the degree of saturation only [9]. However, this mathematical model was criticized by Sridharan (2005) since Pandian et al. (1997) did not consider the influence of the plastic limit. Sridharan (2005) showed that for soils that have similar liquid limit but different plastic limit the reduction on the optimum moisture content diverges from the suggested model as shown in Figure 2.2.

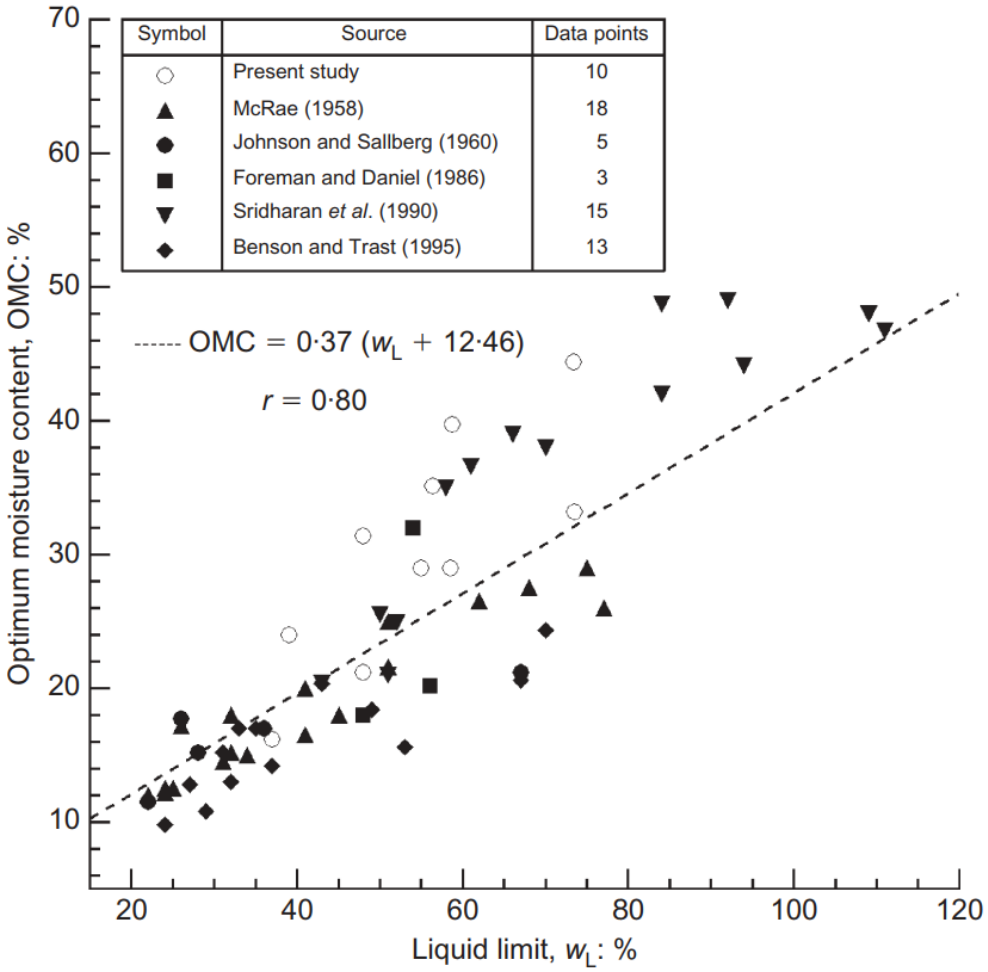

Figure 2.2: Optimum moisture content against LL [10].

On the other hand, the compaction characteristics are fitted well upon plotting them with respect to plastic limit only. The results show that soils with high plasticity have lower maximum dry density but, higher optimum water content [10], as shown in Figure 2.3.

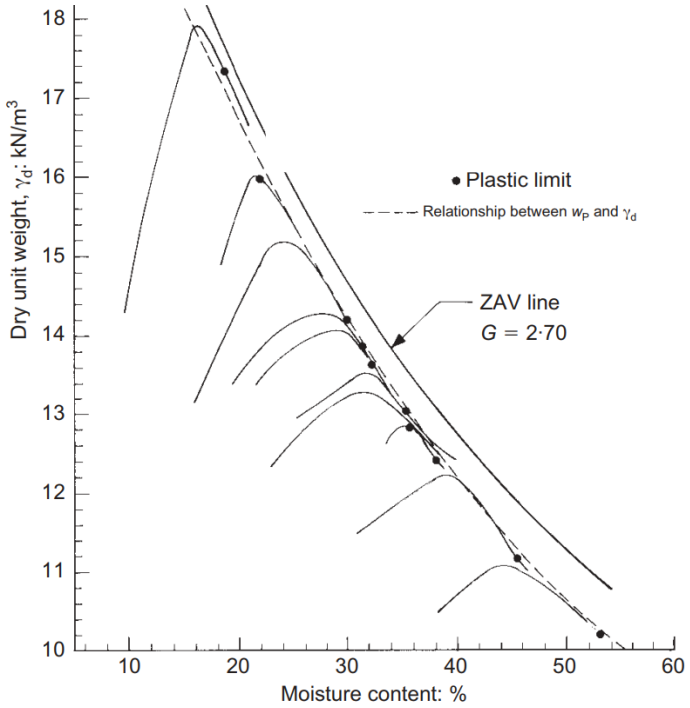

Figure 2.3: The relation between Plastic limit and the compaction characteristics, [10].

2.5 The Effect of Dynamic Compaction on the Unconfined Compressive Strength of Clay

The ultimate stress upon which an unconfined specimen fails under compression is known as the unconfined compressive strength. The unconfined compressive strength parameter is highly influenced by the compaction effort, such as it increases as the compaction effort used in preparing the specimen increases. However, this is only valid if the specimen is prepared at a water content drier than or at the optimum moisture content. On the other hand, if specimen is prepared with moisture content beyond the optimum water content on the wet side of compactor are the behavior of the unconfined compressive strength becomes independent of the compaction effort [11]. The effect of the compaction effort on the unconfined compressive strength of the specimens that are prepared at optimum is presented in Figure 2.4. The unconfined

compressive strength increases non-linearly upon the increment of the compaction effort.

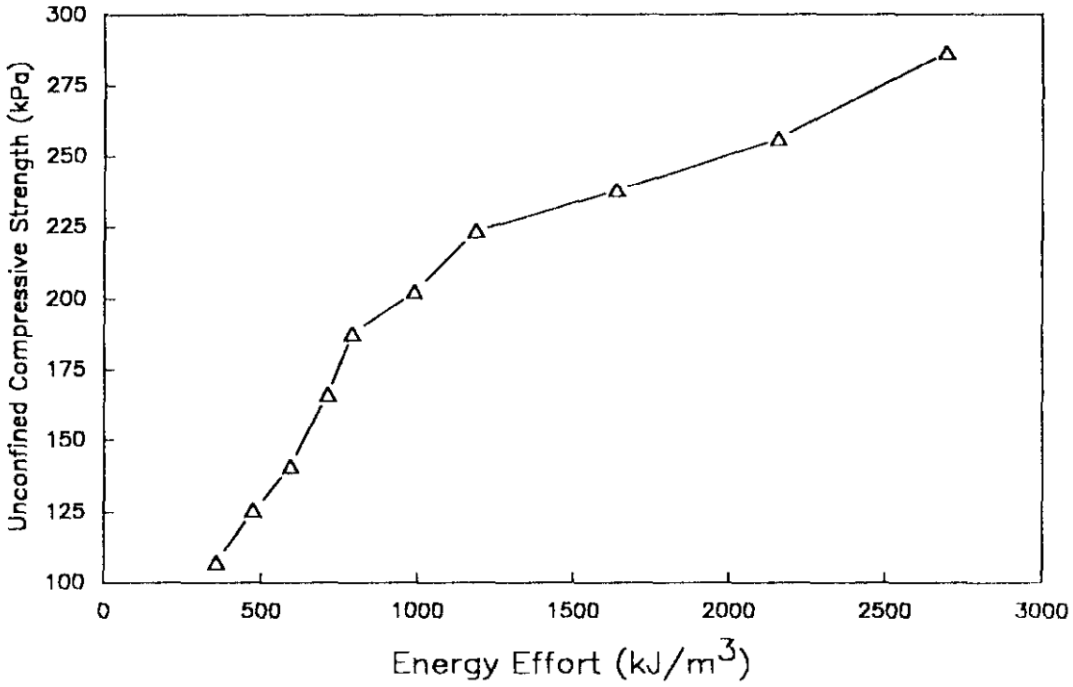

Figure 2.4: The unconfined compressive strength at optimum water content of different compaction efforts. [11]

2.6 The Effect of Dynamic Compaction on Soil Fabric

The fabric of compacted soils is a function of the water content. The soil fabric tends to be randomly arranged (flocculated) when the specimen is compacted on the dry side of optimum. Ultimately, as the compaction water content is increased specimens compacted on the wet side of optimum tend to have well-arranged fabric (dispersed). On the other hand, specimens prepared at the optimum water content will have a combination of flocculated and dispersed fabric [2]. The impact of compaction on the soil fabric is presented in Figure 2.5.

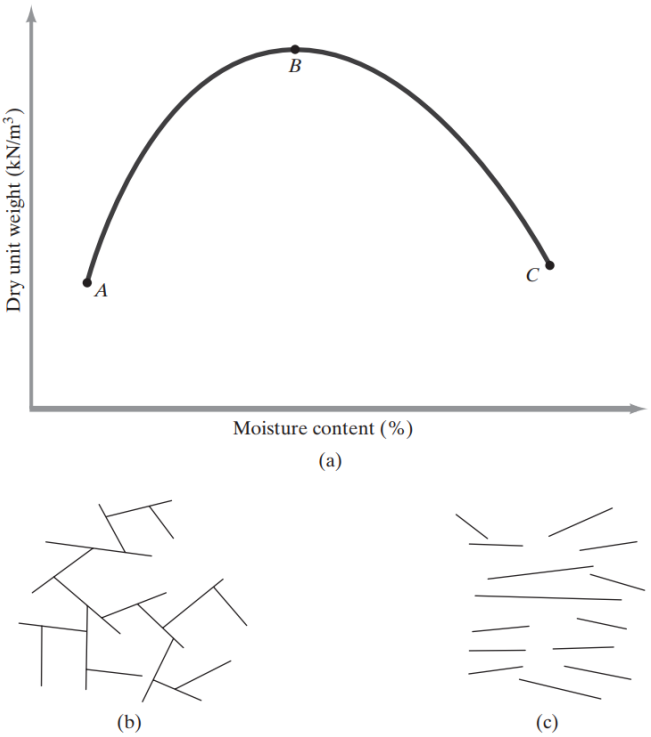

Figure 2.5:(a) Clayey soil compaction curve, (b) Randomly arranged particles on the dry side of optimum, (c) well-arranged particles on the wet side of optimum [2].

2.7 The Effect of Water Content on the Unconfined Compressive Strength of Clay

The water has a major influence on the unconfined compressive strength of clayey soils. The relationship between unconfined compressive strength and the water content follows similar trend to the compaction curve [12]. This behavior can be clearly observed in Figure 2.6. The unconfined compressive strength increases as the water content increases until an optimum value is reached, then drops as the water content continue to increase.

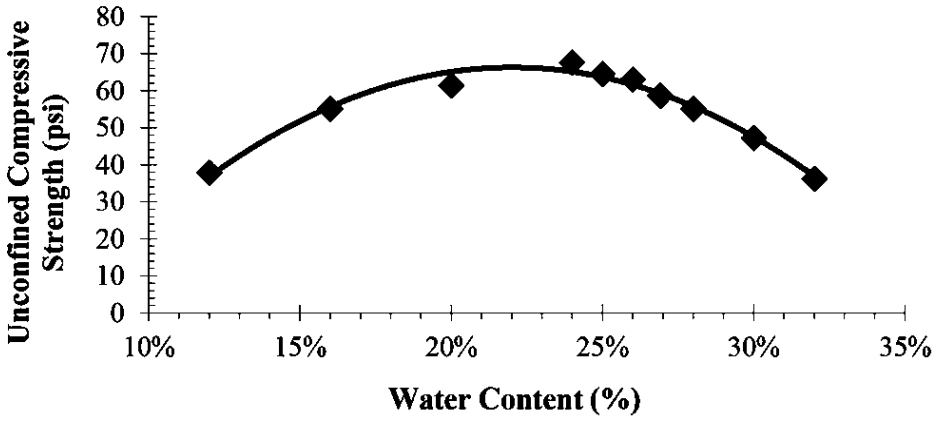

Figure 2.6: The unconfined compressive strength against the water content [12].

2.8 The Influence of Compaction Method on the Undrained Shear Strength of Clay

Wheeler, and Sivakumar, (2000) in their study on the influence of compaction methods (static and dynamic) on the engineering properties of compacted clay concluded that the undrained shear strength was independent of the compaction method as long as the compacted specimens have similar densities. However, they only studied compacted specimens prepared at relatively high water content (25%) [13]. Hence, the behavior of the compacted specimens prepared at the dry side of optimum remains unknown.

2.9 The Effect of Compaction Effort and Water Content on the Swelling Pressure

A nonlinear relationship exists between the compaction effort and the swelling pressure of the compacted clay specimen prepared using dynamic compaction methods [11]. This behavior can be clearly seen in Figure 2.7. When the compaction effort increases the swelling pressure increases. However, this is valid for the specimens prepared at the optimum water content and also for the specimens on the dry side of the optimum. On the other hand, if the specimens were prepared at higher moisture content of the optimum, the compaction efforts have no significant influence [11].

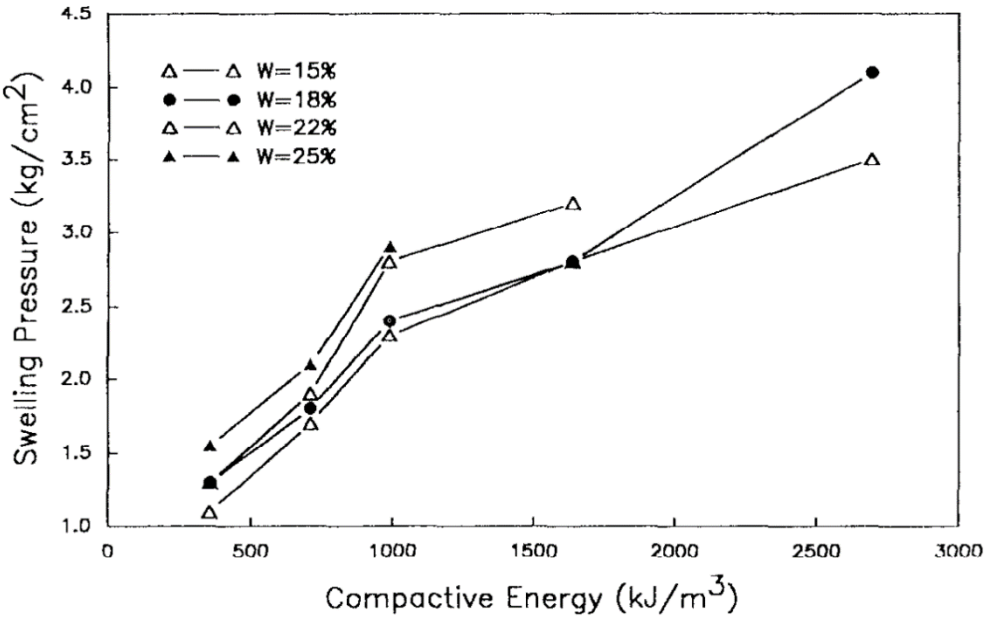

Figure 2.7: The effect of the compaction effort on the swelling pressure of clay [11].

In addition, any increment in the molding water content of the compacted specimens result in a lower swelling pressure in compare with the specimens prepared using the same effort at lower water content [14].

2.10 Effect of soil fabric on the Swelling Behavior of Clay

In a series of centrifuge based swelling tests carried out on highly plastic clay soils with varying soil fabric, Armstrong and Zornberg (2017) observed that the magnitude of primary swell of insitu and compacted specimens is independent of the fabric as long as the specimens have the same moisture content and density. However, the time required to reach the primary swelling varies when the soil fabric is different. For instance, flocculated fabric reduces the time needed for the soil to reach the primary swell since it has higher hydraulic conductivity potential compared with the dispersed fabric [15].

2.11 The Effect of Molding Water Content on the Compressibility Parameters

The specimens prepared at different water content at the same compaction effort show almost no significant variation in terms of compressibility virgin and rebound curves [16]. This can be clearly observed in Figure 2.8. As seen in the figure, all specimens have the same virgin curve and have almost the same final void ratio. The only differences were in the initial void ratio where drier specimens have higher initial void ratio compare with wet specimens.

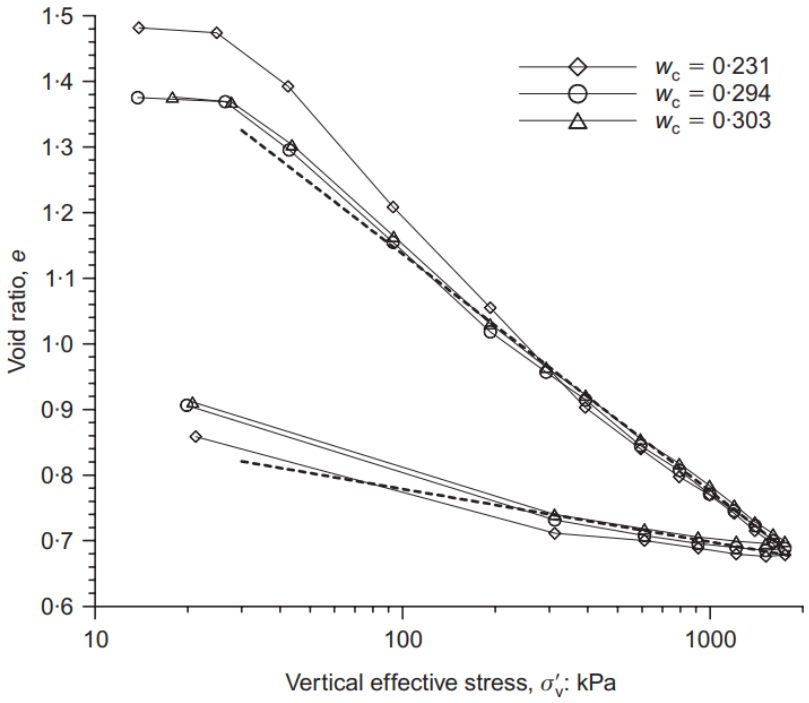

Figure 2.8: Compressibility test results on clay specimens compacted at different initial water contents [16].

2.12 The Electrical Resistivity of Dynamically Compacted Specimens

The ability to oppose the flow of electrical current through a given material is known as electrical resistivity. Ohm-meter (Ωm) is designated as the measuring unit of electrical resistivity in accordance with the metric system. This property of

compromising the flow of the electrical charges can be considered as basic property of any substance [17]. Electrical resistivity of soil can be influenced by many factors, including the chemical composition of the pore fluid, the degree of saturation of the specimen, the porosity, the soil mineralogy, the particles sizes, shape and surface charges and the temperature [18]. The electrical resistivity is tremendously influenced by the pore fluid conductivity, the porosity of the compacted specimen, and the pore's solids and structure. It has been concluded in accordance with Archie's law [19] that the relation between the pore fluid conductivity and the electrical resistivity of soils is inversely proportional. As the pore fluid conductivity increases the resistivity of the compacted soil diminishes [20].

Abu-Hassanein (1996) studied the influence of compaction effort on the electrical resistivity of 10 different soil groups. He found that the relation between the electrical resistivity and the degree of saturation of the compacted specimen is inversely proportional. As the saturation of the compacted specimen increases, the electrical resistivity is reduced. The relation between the electrical resistivity with respect to the degree of saturation is presented in Figure 2.9.

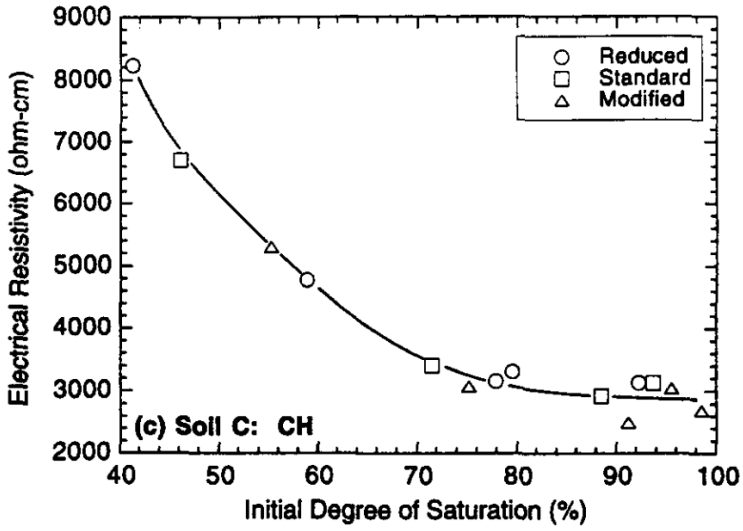

Figure 2.9: The ER with respect to degree of saturation under different compaction efforts [20].

As shown in Figure 2.9 all the points can be fitted together although the soil is compacted under different compaction efforts. Abu-Hassanein (1996) concluded that the electrical resistivity is independent of the compaction effort at a given degree of saturation [20].

The magnitude of positive cations that is required to neutralize the net negative charge of a soil medium is known as the cation exchange capacity [18]. Electrical resistivity is significantly influenced by the cation exchange capacity of the minerals within the body of the compacted specimen. This can be clearly observed in Figure 2.10. As the cation exchange capacity increases the electrical resistivity of the compacted specimen is reduced [21].

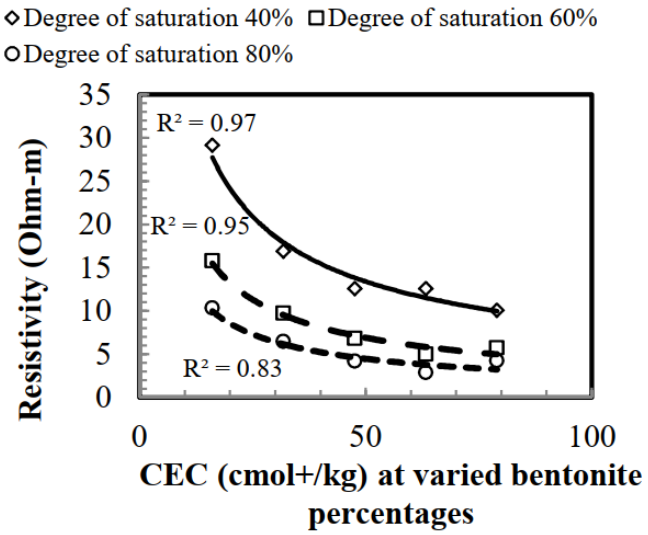

Figure 2.10: The relation between the electrical resistivity and the CEC of compacted specimen under different saturations [21].

The reduction in ER upon the increment of the CEC might be due to the dissolution of the ions and cations that surround the double diffuse layer of the clay mineral within the pore fluid of the specimen.

Chapter 3

MATERIALS AND EXPERIMENTAL METHODS

3.1 Introduction

The previous two chapters of this thesis went through the introductory parts of the research. The following chapter presents the materials used and experimental methods adopted for the study of the influence of compaction energy on the engineering characteristics of selected local fill materials. A series of laboratory tests are also planned to investigate how different methods of compaction affect the engineering properties of the selected soils. All laboratory tests are conducted in accordance with the American Society for Testing and Materials standards (ASTM). The methods followed for sample preparation and measurement of electrical resistivity are explained in detail.

3.2 Experimental soils

In order to make the research more comprehensive, two soils are selected with a large gap among their Atterberg limits and the particle size distributions. The selected soils are also distinguished in terms of their color after being dried and mechanically pulverized. Both soils are abundant in the city of Famagusta, Cyprus.

3.2.1 Alluvial Clay Sample

The alluvial clay sample is widely present at shallow depth in the south campus of the Eastern Mediterranean University (EMU). Large parts of Cyprus are extensively covered with the alluvial deposits such as Nicosia, Famagusta Bay, and both eastern and western shores. These alluvial soils contain high concentration of montmorillonite

minerals that are linked to smectite group [22]. These soils show high strength during dry conditions. Nevertheless, this strength is dramatically reduced during wet seasons [22]. Furthermore, in moist condition the alluvial soil has a brown color. However, when it is dried and pulverized it tends to exhibit a yellowish color. The sample of this soil is obtained from a depth of 3 m from ground surface using a backhoe excavator. Bulk samples are placed in plastic bins and transported to the Soil Mechanics Laboratory at EMU. The approximate sampling location is presented in Figure 3.1.

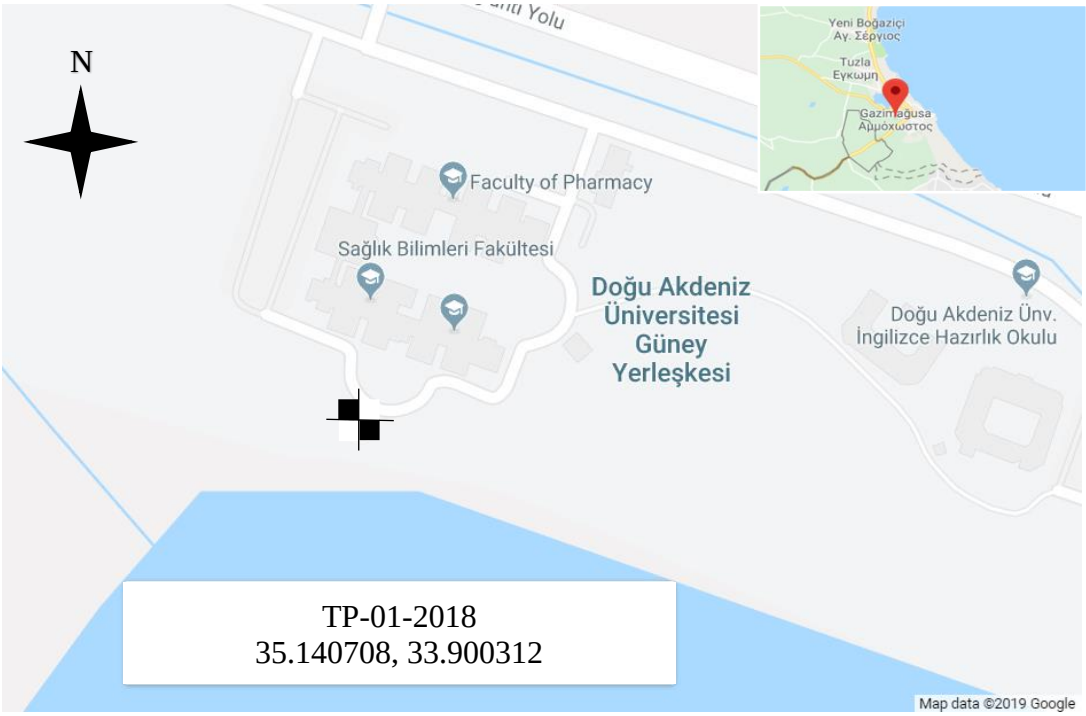

Figure 3.1: Alluvial clay sampling location (Google, 2019).

3.2.2 Terra-Rossa Soil Sample

Terra-Rossa soils are formed through the chemical weathering of limestone and dolomite rocks in karstic regions. Unlike the parent materials this soil has a consistent red color. This red color can be linked to the formation of iron oxides (hematite minerals, Fe_2O_3). It has high permeability and a wide range of particle size distribution [23]. This soil sample is collected from a borrow pit located near Tuzla region, in

Famagusta district. Bulk samples from this soil is collected from the soil heaps using shovels and placed in plastic bins and transported to the Soil Mechanics Laboratory at EMU. The approximate sampling location is presented in Figure 3.2.

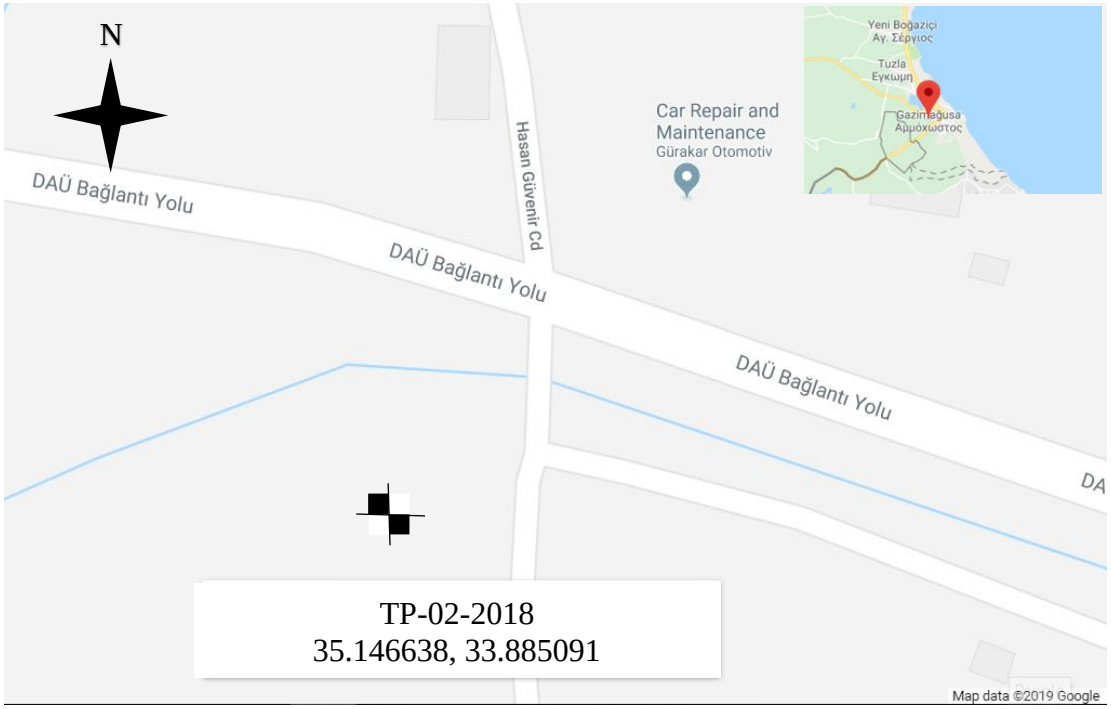

Figure 3.2: Terra-Rossa soil sampling location (Google, 2019).

3.3 Testing Strategy

In order to account for the impact of physical properties in the soil compaction, two types of soils are selected with significant differences among their plasticities (high and low), mineralogy and particle size distribution [22, and 22]. Both dynamic and static compaction methods are implemented, with laboratory program to simulate various compaction for compacted soils analysis. In addition, the influence of moisture content on the compaction performance and engineering characteristics are considered. The arrangement of the testing program is presented in Figure 3.3.

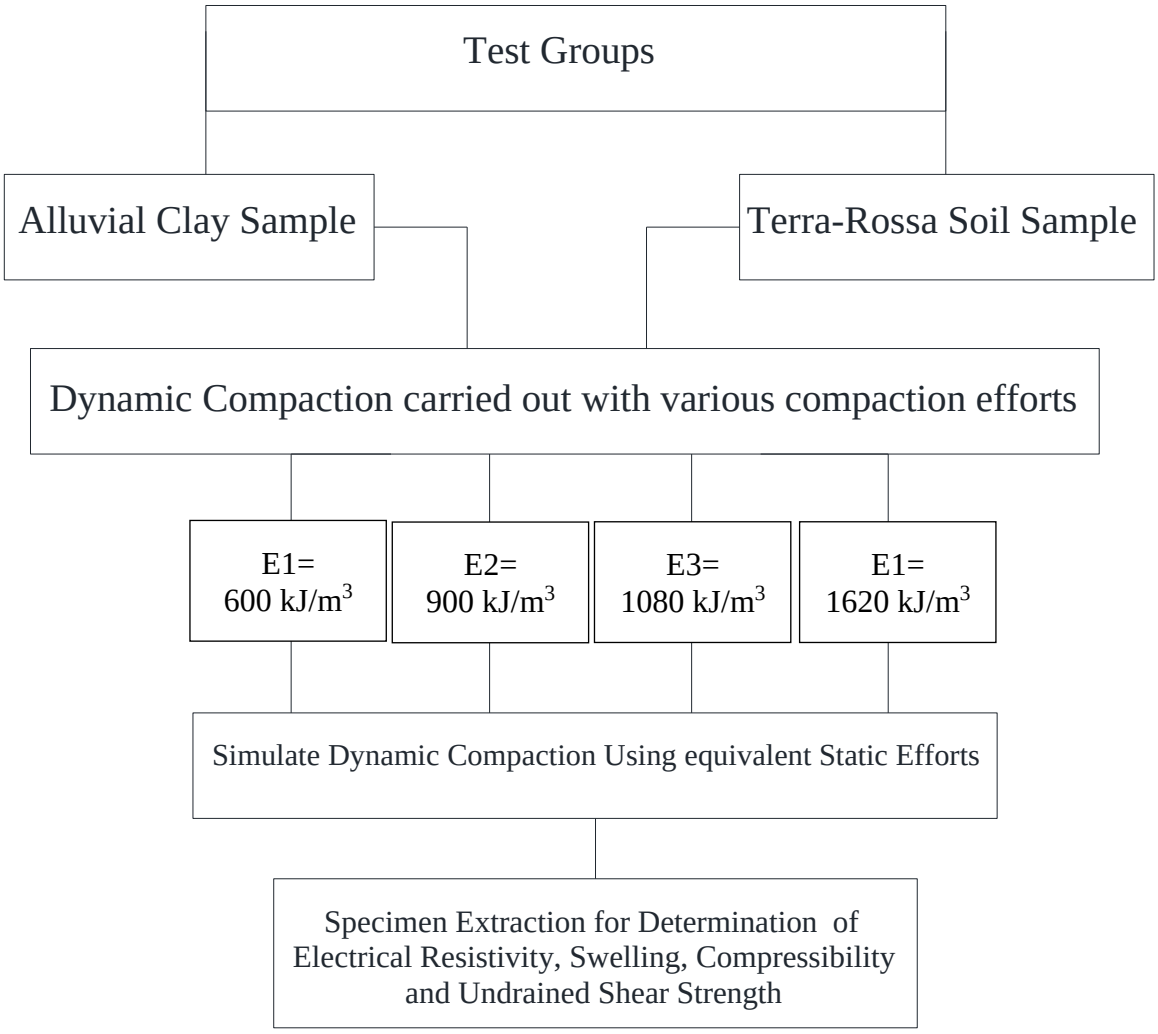

Figure 3.3: Testing program.

3.4 Physical Properties

This part of the dissertation presents in very detailed manner the tests procedures followed together with the adopted methods for data interpretation and curve fitting.

3.4.1 Specific Gravity

ASTM D854-14 is followed for measurement of the specific gravity of the tested soils. The soil specimens are oven dried at 110℃ and mechanically pulverized before conducting the test. The only deviations from the standard are; the Pycnometer capacity, where 100 mL Pycnometer was used, and also the soil specimens are soaked

in distilled water for 3 days before applying the vacuum pressure for removal of trapped air from the voids.

3.4.2 Particle-Size Distribution

In order to determine the particle size distribution hydrometer analysis is carried out in accordance with ASTM D7928-17. The soil specimens are oven dried at 110℃ and pulverized before conducting these tests. These tests are carried out in a temperature controlled room (approximately 24℃), to ensure a consistent climate throughout the sedimentation process. Figure 3.4 shows the particle size distribution of both yellow and red soils. The classifications of particles fractions are presented in Table 3.1.

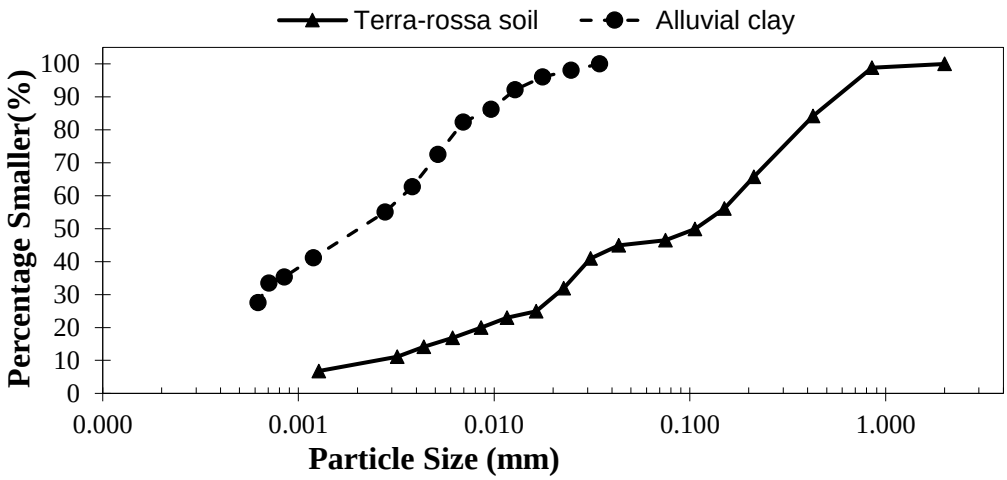

Figure 3.4: Particle size distribution of both Alluvial and Terra-rossa soils.

Table 3.1: classification of particles fractions of Alluvial and Terra-rosa soils.

Soil type	Sand fraction (%)	Silt fraction (%)	Clay fraction (%)
Alluvial clay	0.4	49.6	50.0
Terra-rosa soil	53.5	38.1	8.4

3.4.3 Plasticity Tests

The liquid limit (LL) of the soil specimens are measured using the Casagrande device. The oven dried and pulverized soil specimens are mixed with distilled water at varying proportions and placed in sealed plastic bags for overnight. This method allows for a uniform paste to be formed. After the results are obtained, the water content versus the number of drops plots are interpreted using the least squares method with logarithmic regression. On the other hand, the plastic limit of the soil specimens is measured using the classical method by rolling approximately 2 g of the specimen (prepared for the liquid limit) on a glass board until it fails to reach the 3.2 mm diameter or the formation of the hairline cracks upon rolling is detected. Both tests are conducted in accordance with ASTM D4318-17. The relationship between moisture content and the number of drops obtained in liquid limit test are plotted in semilogarithmic scale in Figure 3.5. and the summary of results for the liquid limit, plastic limit and plasticity index are presented in Table 3.2. From the obtained results it is clearly seen that Alluvial soil specimen has higher plasticity compared to Terra-rosa soil specimen. This can be largely linked to the variation in the clay content of the soil.

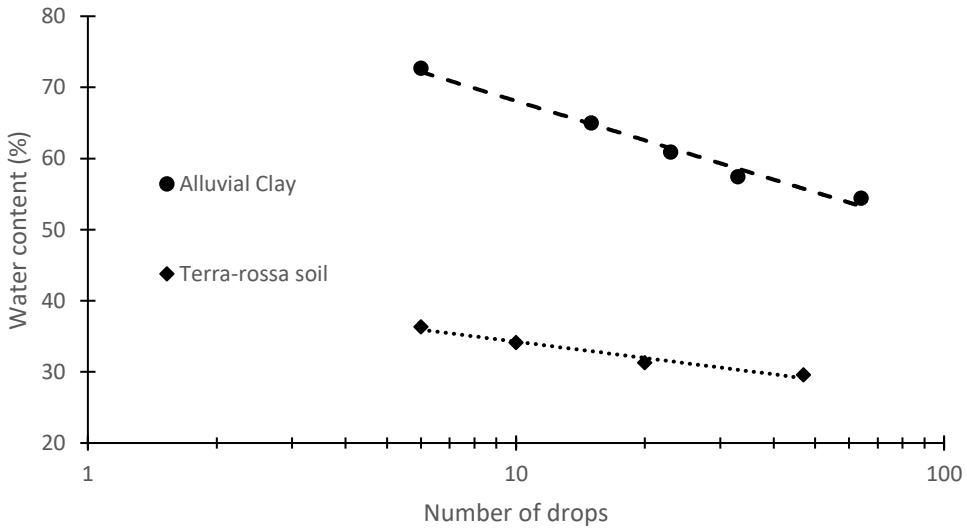

Figure 3.5: Liquid limit test results

Table 3.2:Physical properties of both soils.

Soil type	LL (%)	PL (%)	PI (%)	Classification*	Gs
Alluvial	60.6	30.5	30.1	CH	2.73
Terra-rosa	31.2	19.3	11.9	SC	2.66

* According Unified Soil Classification System (ASTM D2487-17).

3.4.4 Dynamic Compaction

The oven dried and pulverized soil specimens are mixed with distilled water at various proportions and placed in sealed plastic bags for 24 hrs. The standard compaction mold with a diameter of 10.15 cm and height of 11.53 cm is used. The soil specimens are compacted in three layers in accordance with ASTM D1557-12. The dynamic compaction is performed using mechanical compactor in the Soil Mechanics Laboratory. The mechanical compactor offers two different drop heights for the compaction hammer (12 in and 18 in). In addition to this, the machine main hammer, which weighs 2.5 kg can be equipped with an extra 2 kg steel rod resulting in a total weight of 4.5 kg. As a result, four different compaction efforts can be conducted.

The kinetic energy formed just before the impact time can be calculated using Equation 3.1 and Equation 3.2. In these equations the drag force exerted on the hammer surface is neglected as the drop height (h_D) is relatively small and the acceleration is assumed to be equal to the gravitational acceleration [24]. Ultimately, the compaction effort can be calculated as presented in Equation 3.3

$$K_e = \frac{1}{2} m_h {v_{im}}^2 \quad (3.1)$$

$$v_{im} = \sqrt{2gh_D} \quad (3.2)$$

$$E_n = \frac{K_e N_b N_l}{V} \quad (3.3)$$

where,

K_e: kinetic energy (J).

m_h: mass of the hammer (kg).

v_{im}: velocity of the hammer just before the impact (m/s).

g: gravitational acceleration (m/s^2).

h_D: drop height (m).

E_n: compaction effort.

V: volume of the compaction mold.

N_b: number of blows.

N_l: number of layers.

The compaction efforts applied in this research are presented in Table 3.3.

Table 3.3: Dynamic compaction efforts.

Effort	**E1**	**E2**	**E3**	**E4**
$\boldsymbol{m_h}$ **(kg)**	2.5	2.5	4.5	4.5
$\boldsymbol{h_D}$ **(m)**	0.3048	0.4572	0.3048	0.4572
Number of drops	25	25	25	25
Number of layers	3	3	3	3
$\boldsymbol{K_e}$ **(J)**	7.48	11.21	13.46	20.18
Total compaction effort (kJ/m^3)	601.3	901.2	1082.1	1622.3

Dynamic Compaction Characteristics Determination

The relationship between dry density and water content can be best fitted using polynomial function as compaction curves typically have a nonlinear bell-shaped form. Hence, least squares method with 3rd degree polynomial regression is followed in the analysis of the compaction characteristics. The typical form of the fitting function used in the data analysis is presented by Equation 3.4

$$\rho_d = a + b\,w_c + c\,w_c^2 + d\,w_c^3 \qquad (3.4)$$

where,

ρ_d: dry density in (g/cm^3).

w_c: water content.

$a, b, c, and\ d$: polynomial coefficients, which can be determined by using Microsoft Excel.

The maximum dry density ($\rho_{d\,max}$) and the optimum water content (w_{opt}) are evaluated by solving the first derivative of the fitting function for the water content by equating it to zero. The general form of the derivative is presented by Equation 3.5, and the schematic presentation of the result is shown in Figure 3.6.

$$\frac{d\,\rho_d}{d\,w_c} = b\ + 2 \times c\,w_c + 3 \times d\,w_c^2 \qquad (3.5)$$

The compaction curves obtained for Alluvial clay and Terra-rosa soil specimens are presented in Figure 3.7 and Figure 3.8 respectively. The results of maximum dry density and optimum water content obtained from the curves are presented in Table 3.4. It can be observed that Terra-rosa soil has higher dry density and lower optimum water content. This can be explained by the lower plasticity and the wider particle size

distribution for the soil. The Terra-rosa soil is comprised of a wider range of particle sizes compared to the Alluvial clay, which is only composed of silt and clay.

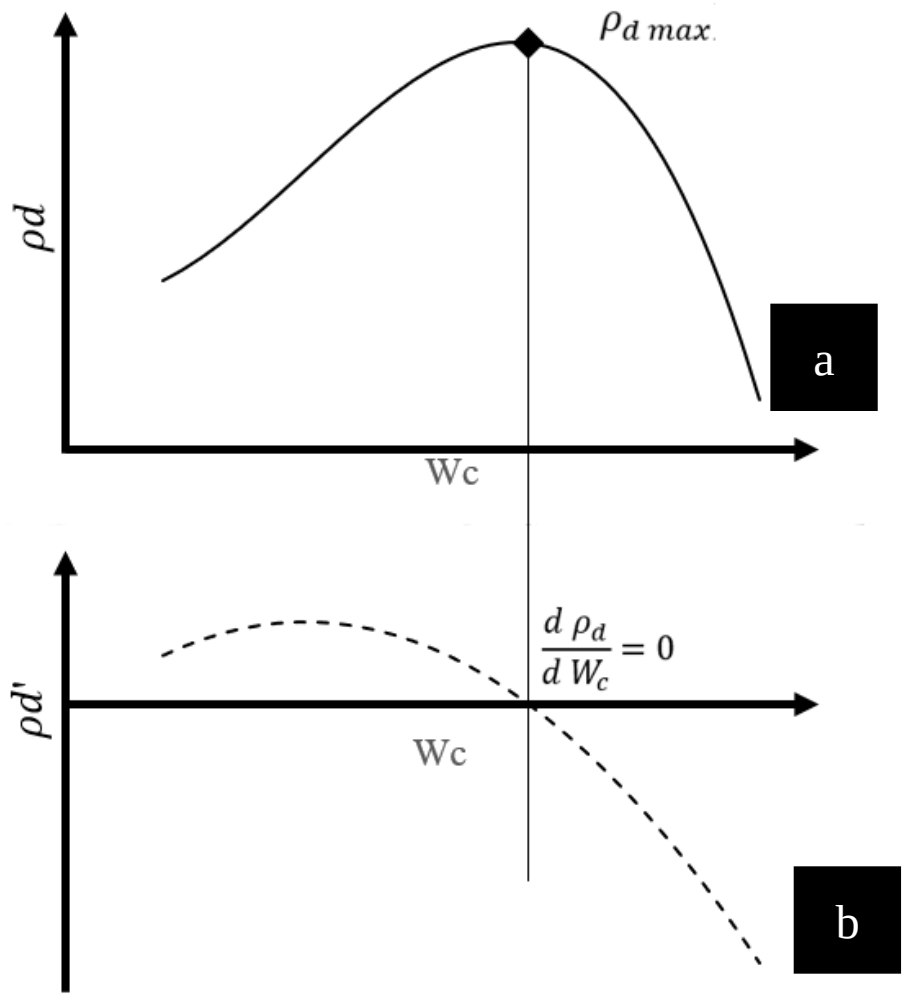

Figure 3.6: (a) The compaction characteristics curve and (b) The derivative of the compaction characteristics curve with respect to water content.

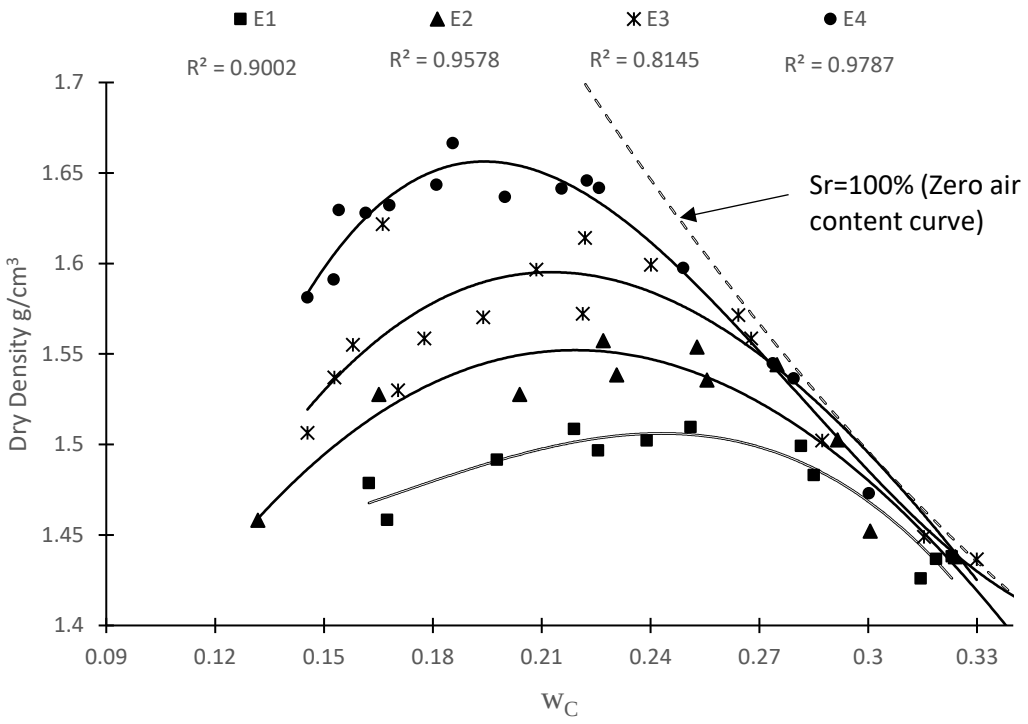

Figure 3.7: Compaction curves for Alluvial clay

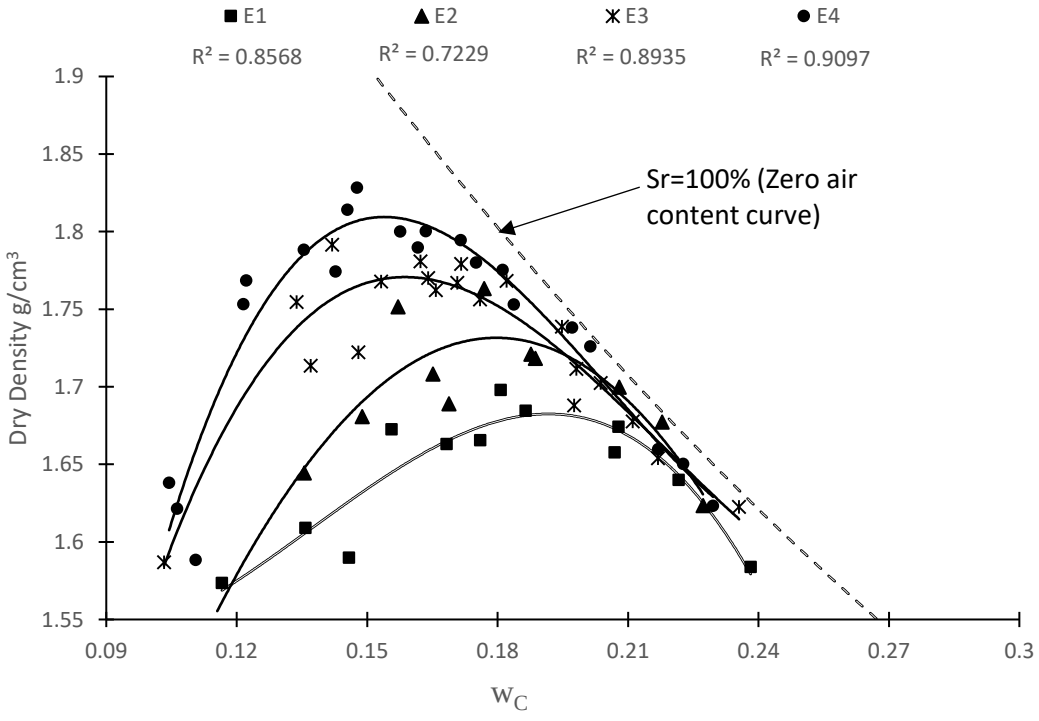

Figure 3.8: Compaction curves for Terra-rossa soil.

Table 3.4: Maximum dry density and optimum water content of both soils at different compaction efforts.

	Alluvial clay		Terra-rosa soil	
Compaction effort	w_{opt} (%)	ρ_{dmax} (g/cm^3)	w_{opt} (%)	ρ_{dmax} (g/cm^3)
E1	24.3	1.51	19.1	1.682
E2	21.9	1.552	17.5	1.735
E3	19.6	1.628	15.8	1.77
E4	19.1	1.646	15.5	1.809

3.4.5 The Static Compaction

The densities obtained in the dynamic compaction tests are simulated using static effort for the comparing of engineering behavior in other tests. The test setup is shown in Figure 3.9. The compression is performed using the California Bearing Ratio (CBR) test apparatus, and the required force to reach the targeted density is measured using the loading ring attached to this equipment. The static compaction is carried out using the following procedure:

1. After trial and error, it is observed that 500 g of soil is needed for this test, which is collected from the same wet soil patch that is prepared for the dynamic compactions test.

2. The wet soil specimen is placed in a cylindrical steel mold with a diameter of 50 mm and height of 210 mm.

3. The soil specimen is compressed with the penetration of a steel prob at a constant rate of 1.27 mm/min (standard CBR testing speed) until the target density equivalent to the dynamic compaction density is attained.

The required penetration of the CBR rod into the soil during compression can be calculated as shown by Equation 3.6.

$$L_p = H_m - H_t = H_m - \frac{m_{ws}}{A \times \rho_{bulk}} \quad (3.6)$$

Where,

L_p: length of penetration (cm).

H_m: mold full height (cm).

H_t: target height (cm).

m_{ws}: mass of wet soil (g).

A: cross-sectional area of the mold ($A = \pi \times D^2/4$ cm^2).

ρ_{bulk}: target density (from dynamic compaction g/cm^3).

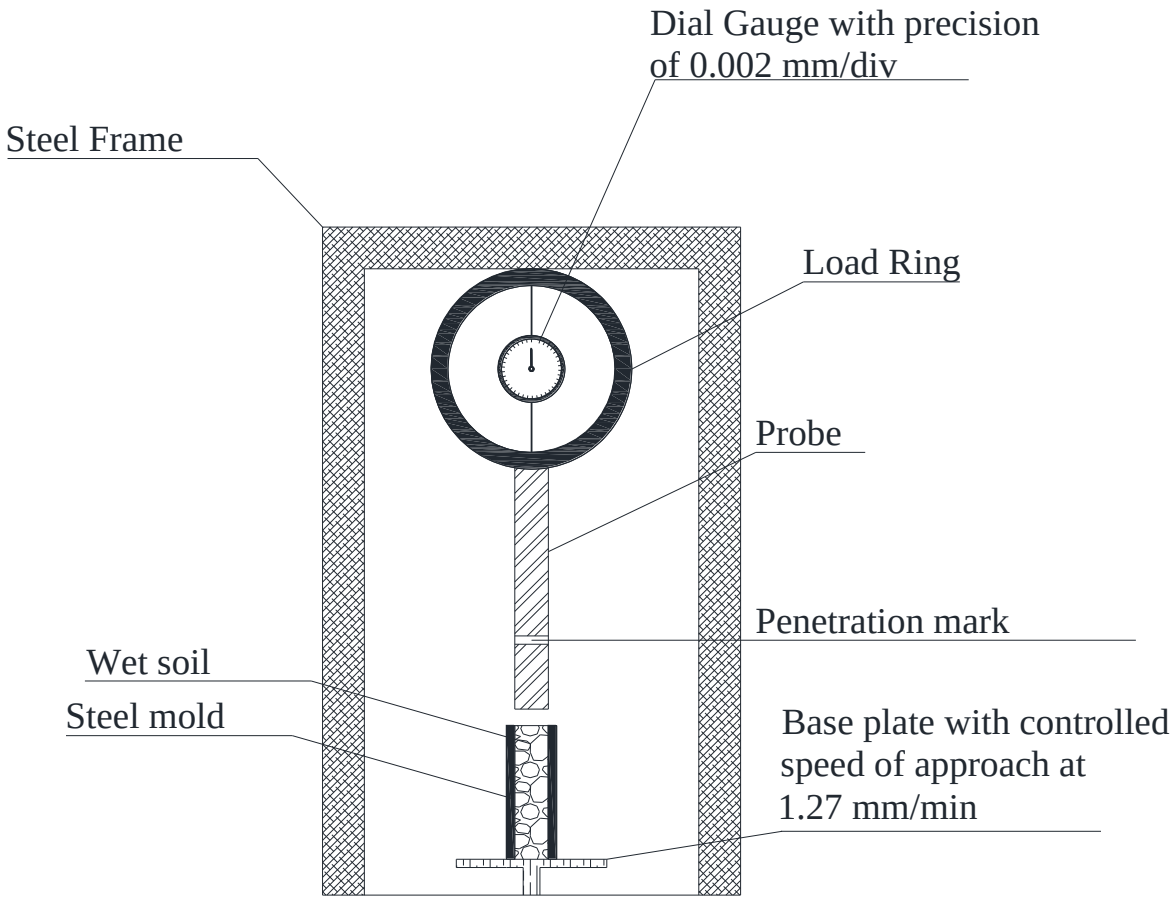

Figure 3.9: Static compaction test setup.

3.4.6 Sample Extraction

A thin walled steel soil sampler (1.2 mm thickness) is pushed slowly into the compacted soil using a motorized hydraulic jack to obtain sub-specimens from compacted specimens as shown in Figure 3.10. Only one specimen per compacted sample is obtained to prevent sample disturbance. The sampler interior diameter and the height of the sampler used are 50 mm and 102 mm respectively. The extracted soil specimen is immediately sealed with stretch film to prevent moisture loss and placed in vacuum desiccator.

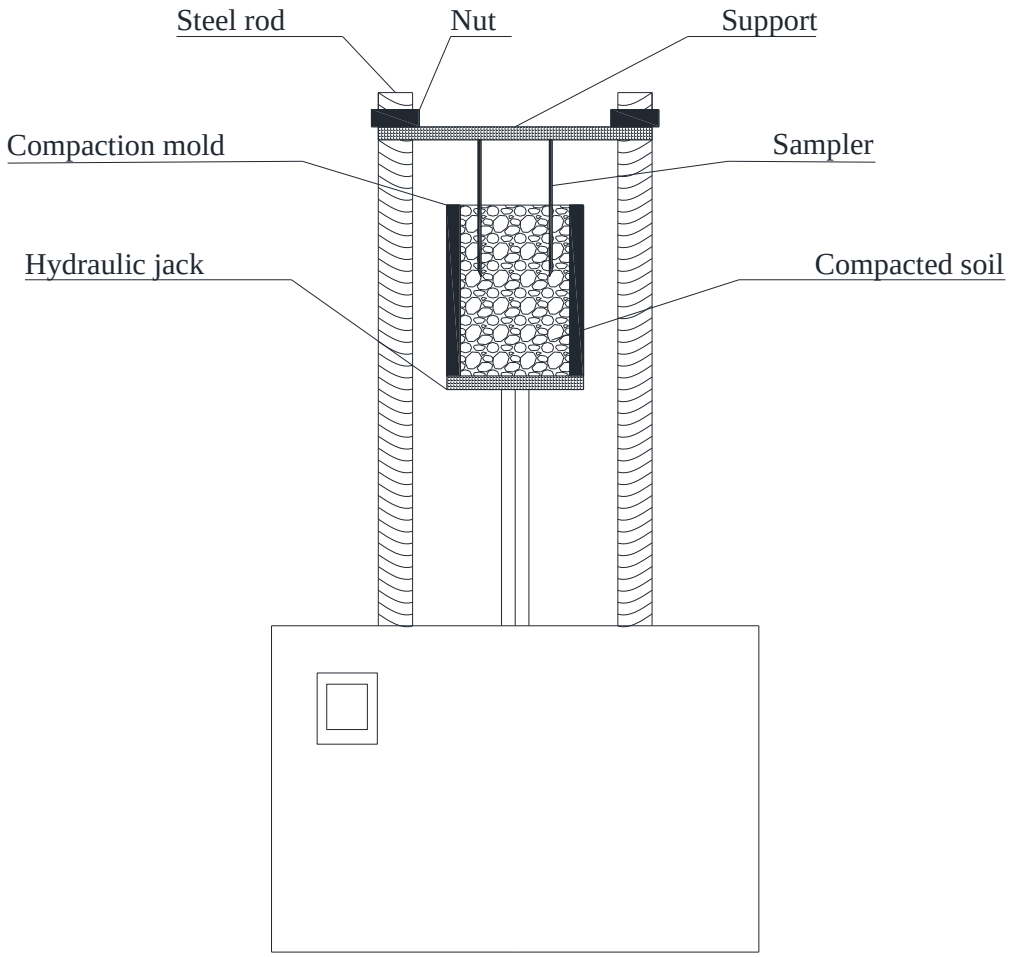

Figure 3.10: Extraction of specimens with the help of hydraulic jack.

3.4.7 Soil Properties Using Phase Relationships

After extracting the specimens average height and diameter are measured with a sensitive caliper (0.01 mm) in order to calculate the phase relation parameters in a precise manner. Also, the mass of each specimen is recorded and the water content is reviewed from trimmings. The soil properties using phase relationships are calculated as illustrated in the following equations

• Degree of Saturation, (Sr)

The degree of saturation is calculated by dividing volume of moisture within the specimen to the volume of voids as shown in Equation 3.7.

$$Sr = \frac{V_w}{V_v} = \frac{\frac{m_w}{\rho_w}}{V - V_s} = \frac{\frac{m_w}{\rho_w}}{V - \frac{m_s}{Gs}} = \frac{\frac{m_w}{\rho_w}}{V - \frac{\frac{m_t}{1 + w_c}}{Gs}}$$

$$= \frac{m_w}{\rho_w \left(V - \frac{m_t}{Gs(1 + w_c)} \right)} \tag{3.7}$$

• Porosity, (n)

The porosity of specimen is computed by dividing the volume of voids on the total volume as shown in Equation 3.8.

$$n = \frac{V_v}{V} = \frac{V - \frac{\frac{m_t}{1 + w_c}}{Gs}}{V} = 1 - \frac{m_t}{Gs\, V(1 + w_c)} \tag{3.8}$$

• Void ratio, (e)

The void ratio of the specimen is calculated by dividing the volume of voids to the volume of solids as shown in Equation 3.9.

$$e = \frac{V_v}{V_s} = \frac{V - \frac{\frac{m_t}{1+w_c}}{Gs}}{\frac{m_t}{\frac{1+w_c}{Gs}}} = \frac{V}{\frac{m_t}{\frac{1+w_c}{Gs}}} - 1 = \frac{Gs}{\rho_d} - 1 \quad (3.9)$$

where,

Sr: degree of saturation.

n: porosity of the specimen.

e: void ratio of the specimen.

V: total volume of the specimen (cm^3).

V_v: volume of voids within the specimen (cm^3).

V_w: volume of water within the specimen (cm^3).

V_s: volume of solids within the specimen (cm^3).

m_t: bulk mass of the specimen (g).

m_s: dry mass of the specimen (g).

m_w: mass of water within the specimen (r).

ρ_w: density of water at 23℃ (0.997 g/cm^3).

Gs: specific gravity of the soil.

w_c: water content.

3.4.8 Electrical Resistivity Measurement

The electrical resistivity of the compacted soil specimens is measured using the four probes technique [25]. This test is basically an electrical circuit comprised of an AC adapter, wiring, compacted soil specimen, and a resistor (2300 Ω) as shown in Figure 3.11. An alternating current was adopted since direct current may initiate reactions among the soil minerals, water and the probes themselves affecting the stability of the readings. In addition, to prevent the variations due to thermal changes all specimens are tested in a temperature-controlled room at 23C° (±0.5C°). A highly sensitive electronic voltmeter is used to measure the voltage transmitted through the soil specimen with an accuracy of 0.001 Volt. The electrical resistivity is calculated as shown in Equation 10.

$$ER = \frac{A \times \Delta V}{I \times d_p} = \frac{A \times \Delta V}{\frac{V_d}{\Omega} \times d_p} \tag{3.10}$$

where,

ER: electrical resistivity (ohm-cm).

ΔV: measured voltage transmitted through the compacted specimen (Volt).

Ω: resistor capacity (Ohm).

d_p: distance between electrodes (cm).

V_d: Voltage drop measured at resistor (Volt).

A: cross-sectional area of the compacted specimen (cm^2).

I: current (A).

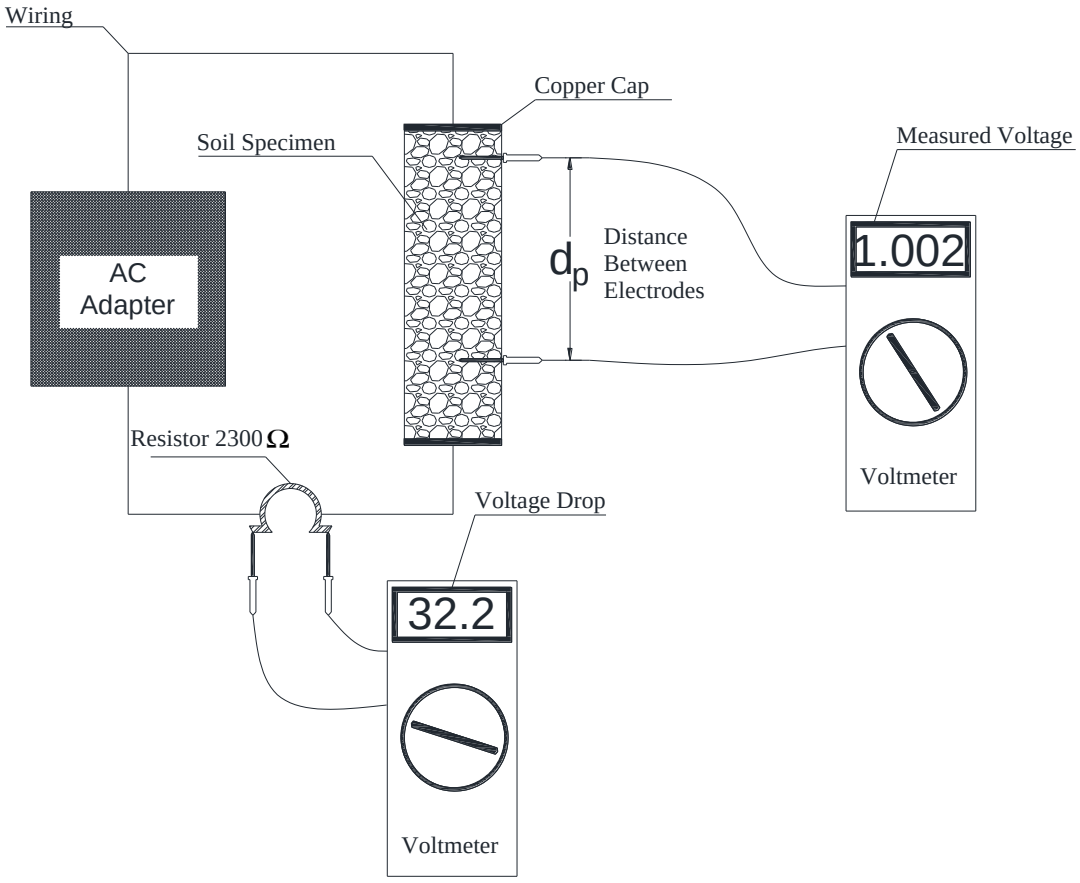

Figure 3.11: Electrical resistivity test setup.

3.4.9 Unconfined Compression Test

All specimens are tested to obtain unconfined compressive strength and undrained shear strength. The specimen dimensions are; diameter of 50 mm and height of 100 mm. The specimens are sheared at a constant rate of 1 mm per minute in accordance with ASTM D2166/D2166M-16. Readings are taken manually every 0.01% of the axial strain until failure. Finally, water content measurement is repeated once again using parts of the failed specimen. The axial stress and axial strain are calculated as presented in Equations 3.11 and 3.12 respectively and plotted for further interpretation. The undrained shear strength is obtained by taking half of the axial stress at failure as shown in Equation 3.13. The initial tangent modulus (E_i) is obtained by taking the slope of the tangent line at 0.1% strain as shown in Figure 3.13. The modulus at 50%

of the ultimate strength is also evaluated by dividing the axial stress to the corresponding axial strain as shown in Equation 3.14.

$$\varepsilon_a = \frac{\Delta H}{H_0} \tag{3.11}$$

$$\Delta\sigma_{corrected} = \frac{\Delta\sigma}{1+\varepsilon_a} \tag{3.12}$$

$$C_u = \frac{\Delta\sigma_{peak}}{2} \tag{3.13}$$

$$E_{50} = \frac{0.5\,\Delta\sigma_{peak}}{\varepsilon_{50}} \tag{3.14}$$

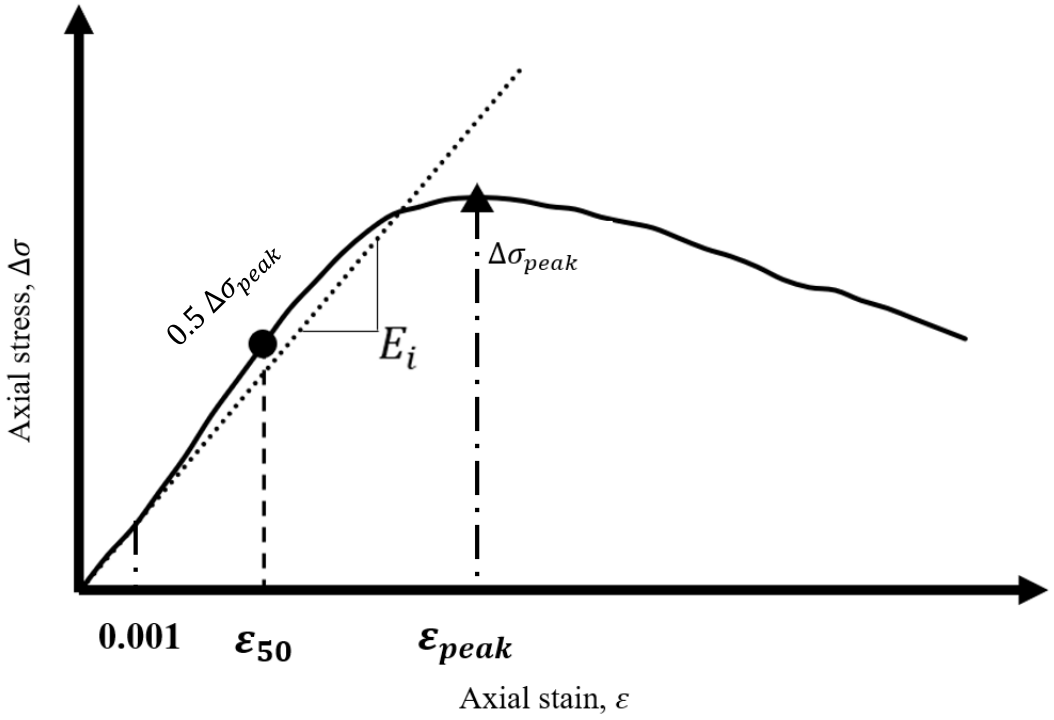

Figure 3.12: The axial stress versus the axial strain diagram of the unconfined compression test.

3.4.10 One Dimensional Consolidation Test

Swelling and compressibility of specimens prepared at optimum water content of the dynamic compaction and static compaction are tested using one dimensional consolidation test. Typical dimension of the test specimens used are; diameter of 50 mm and height of 14.24 mm ($\pm$ 0.2 mm). The tests are conducted and the results are

analyzed in accordance with ASTM D2435/D2435M-11. The initial swelling (saturation) stage is carried until primary swell is completed under 5 kPa surcharge. This stage is followed by an incremental loading procedure, applying consecutive loadings of 0.5, 1, 2, 4, 8, 16, 32, and 64 kg. After the loading part is completed, unloading is started as the following sequence 64,32,16 kg, and 5 kPa.

3.4.11 The Mathematical Model for the Estimation of Preconsolidation Pressure

As one of the research goals is to assess the effect of compaction methods on the preconsolidation stress, a mathematical model for the evaluation of the preconsolidation pressure is used [26]. The mathematical model is suggested by Soltani, et al. (2018). The mathematical model basically fits the test data series during the loading stages using the function given in Equation (3.15) and uses the fitting coefficients to estimate the pre-consolidation pressure. The graphical representation of the mathematical model is presented in Figure 3.13.

$$\frac{\sigma'}{e_0 - e(\sigma')} = \alpha + \beta\sigma' \tag{3.15}$$

where,

σ': applied effective stress (kPa).

e_0: initial void ratio.

$e(\sigma')$: void ratio at given effective stress.

α and β: are fitting parameters.

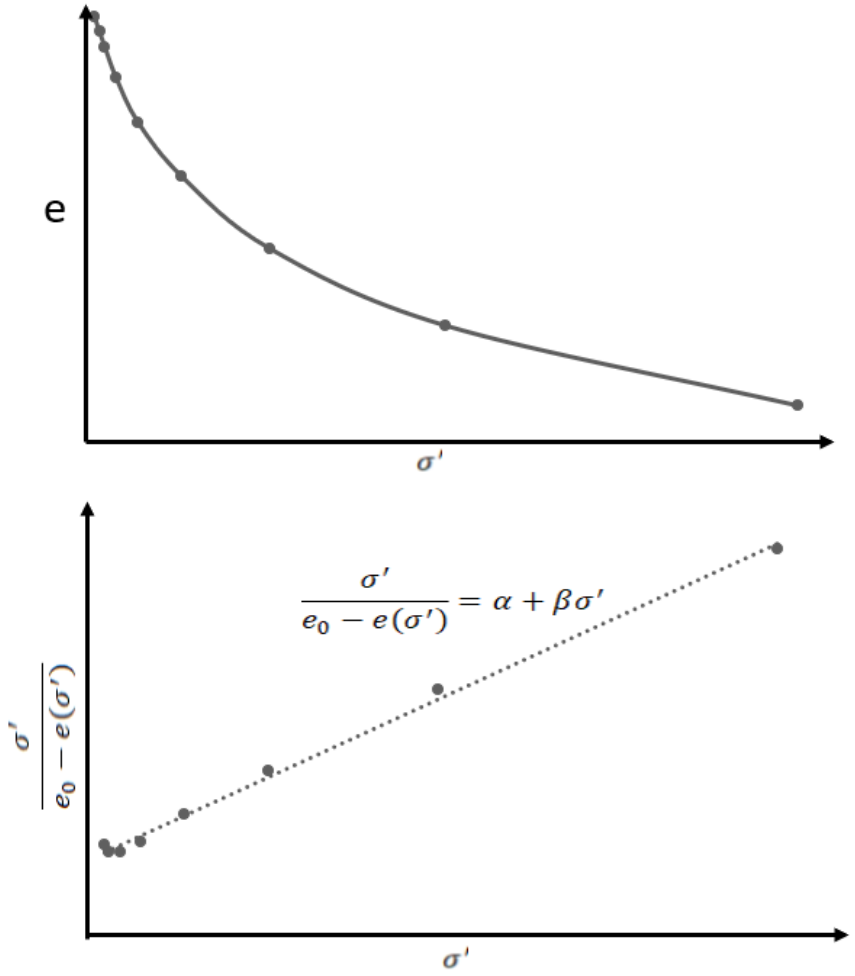

Figure 3.13: The graphical representation of Soltani, et al. (2018) mathematical models.

Chapter 4

RESULTS AND DISCUSSIONS

4.1 Introduction

This chapter of the dissertation presents and discusses the results of the adopted test methodology in a comprehensive manner. The behavior of the compacted soil specimens prepared using dynamic and static compaction efforts are discussed in terms of electrical resistivity, undrained shear strength, the compressibility parameters, and swelling characteristics.

4.2 The Static Compaction Stresses

Since decades researchers tried to determine an equivalent static stress that can represent the maximum dry density and the optimum water content of the standard Proctor compaction test. However, the results were inconsistent and none of which considered neither the dry nor the wet side of optimum [6,5, and 7]. In this section of the study the dynamic compaction curves of 4 different compaction efforts are simulated using static stress for 2 different soil types. The results show that the equivalent static stress is not constant along the compaction curve of a given effort, where the static equivalent stress is rather a function of the moisture content. Ultimately, moisture content will always reduce the equivalent static stress as it increases, since fine grained soil deformability increases upon wetting. The results of the equivalent static stress with respect to the water content for the Alluvial clay and the Terra-rossa soil are presented in Figure 4.1 and Figure 4.2, respectively.

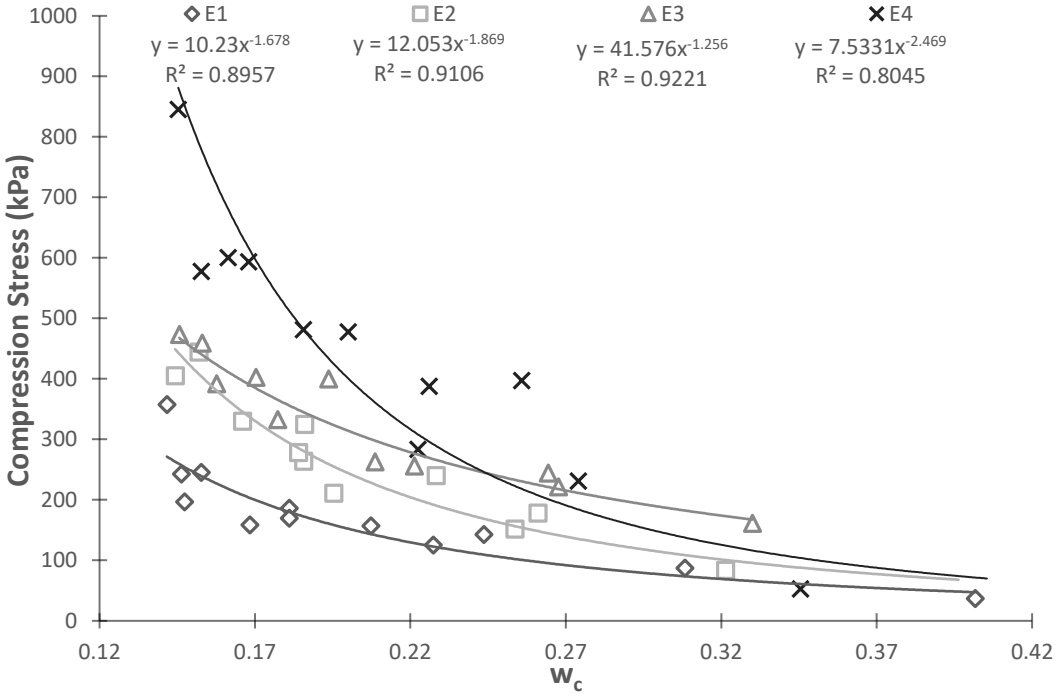

Figure 4.1: The equivalent static stresses of dynamic compaction with respect to w_c of the Alluvial clay.

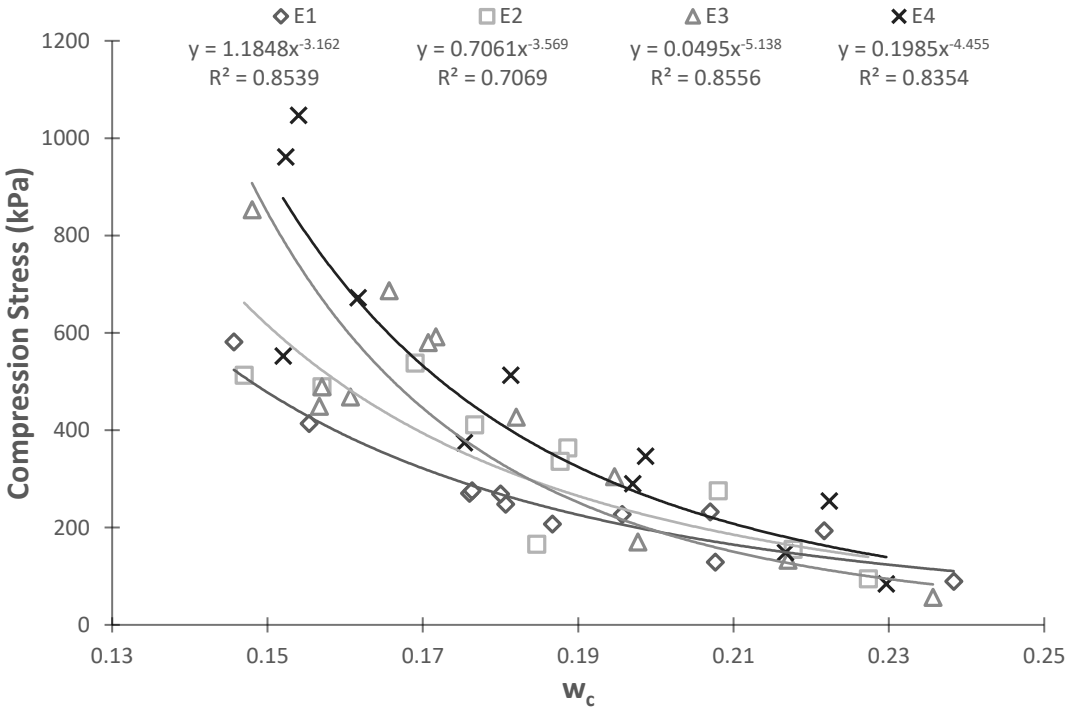

Figure 4.2: The equivalent static stresses of dynamic compaction with respect to wc of the Terra-rossa soil.

The equivalent static stress is highly influenced by the dynamic compaction effort at low water content. However, as the water content increases the equivalent static stress becomes independent of the compaction effort. This can be linked to the fact that, at low water content high dynamic compaction effort results in higher dry density compared with small dynamic compaction effort. On the other hand, at high water content all compaction efforts will result in the same dry density. Additionally, the equivalent static stresses that represent the optimum water content varies significantly with respect to the soil types. These equivalent static stresses at optimum are represented in Table 4.1.

Table 4.1: The static equivalent stress of the dynamic compaction effort at the optimum water content.

Compaction effort	**Equivalent static stresses at optimum (kPa)**	
	Alluvial clay	**Terra-rossa soil**
E1	109	222
E2	205	355
E3	322	648
E4	448	803

The equivalent static stress of the Terra-rossa soil is almost two times the equivalent static stress of the Alluvial clay. This can be explained by the fact the Terra-rossa is a more uniform gradation and lower plasticity. Hence, higher stress is required to reduce the voids within the specimen soil. Ultimately, the obtained stresses are much lower than the stresses presented in Table 2.1. This can be linked to the fact that the mold that is been used in this study has a smaller diameter.

4.3 The Electrical Resistivity

An extensive number of researches are presented in the literature who studied electrical resistivity (ER) of compacted soil specimen, which cover many aspects [18, 19, 20, and 21]. However, the influence of the compaction method is not clearly addressed yet. The following section investigates the influence of compaction method on the electrical resistivity of compacted soil specimens.

4.3.1 Electrical Resistivity in Terms of Water Content

The test results indicated that, the electrical resistivity is inversely proportional to the water content. In other words, as water content increases the electrical resistivity is reduced significantly. On the other hand, as the compaction effort increases the electrical resistivity is reduced for the specimens prepared on the dry side of optimum. Since, higher compaction effort leads to a higher dry density and hence, clay amount for a given specimen, ER is then reduced due to comparably higher concentration of free anions and cations now present in the denser specimen. Ultimately, the ER behavior is independent of the compaction method at high water content, where all compaction efforts result in similar densities hence, similar resistivities. This can be observed in the results of the tested specimens on both soils. The relationship between the electrical resistivity and the water content for the statically and dynamically prepared specimens of Alluvial clay and Terra-rossa soil are displayed in Figure 4.3 and Figure 4.4 respectively.

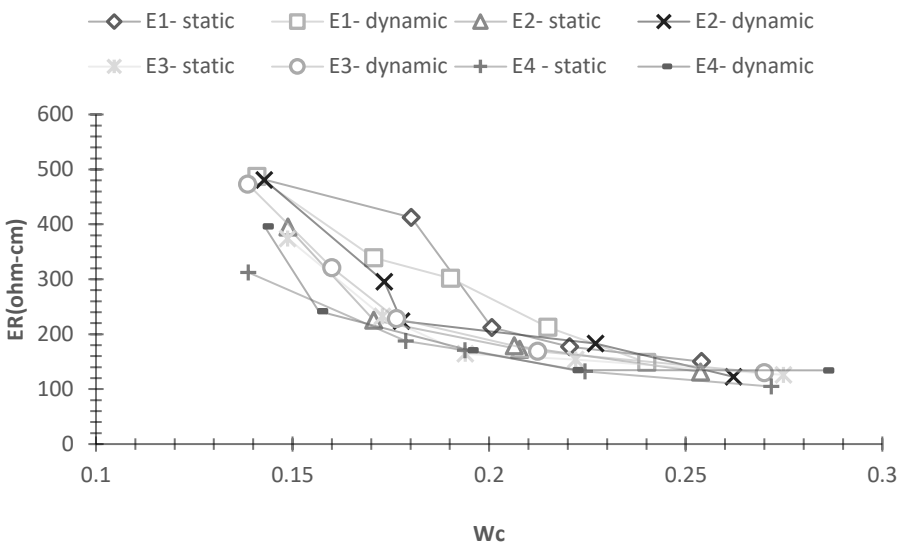

Figure 4.3: The relationship between ER and the water content of dynamically and statically compacted Alluvial clay specimens.

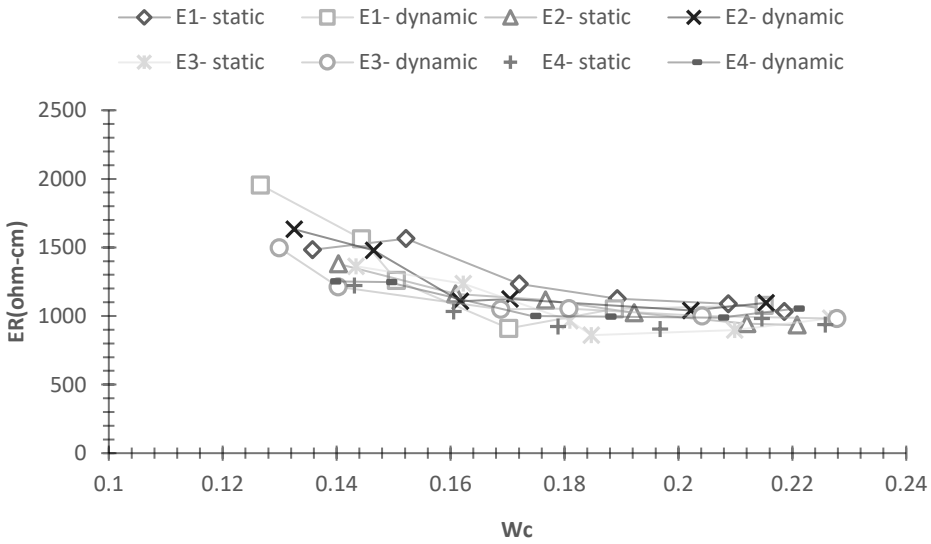

Figure 4.4: The relationship between ER and the molding water content of dynamically and statically compacted Terra-rossa soil specimens.

In addition, the Alluvial clay is highly influenced by the compaction effort unlike the Terra-rossa soils. This can be linked to higher clay mineral content of the alluvial clay specimens, which reduces the electrical resistivity. On the other hand, Terra-rossa soil has a lower clay mineral content, which results in no significant reduction of the electrical resistivity against the increment in the compaction effort.

4.3.2 Electrical Resistivity in Terms of Saturation

The tests results indicate that as the degree of saturation increases, the electrical resistivity is decreased. This is considered to be due to the increase of pore water promoting electrical flow through the pore structure. More interestingly, it is seen from the test results that the relationship between ER and Sr of dynamically compacted clay specimen is independent of the compaction effort, which was also observed by Abu-Hassanein (1996), [20]. This implies that the electrical flow in soils is dominated by the saturation of the pore structure rather than the absolute magnitude of the pore volume [4, 19]. Figure 4.5 and Figure 4.6 present the relationship between ER and Sr under 4 different dynamic compaction efforts for Alluvial clay and Terra-rossa soil respectively.

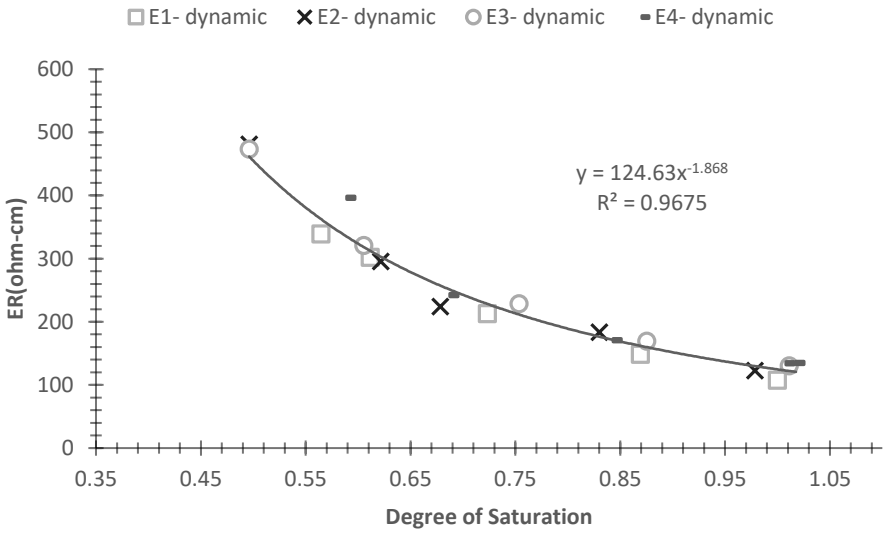

Figure 4.5: The relationship between ER and the degree of saturation of dynamically compacted Alluvial clay specimens.

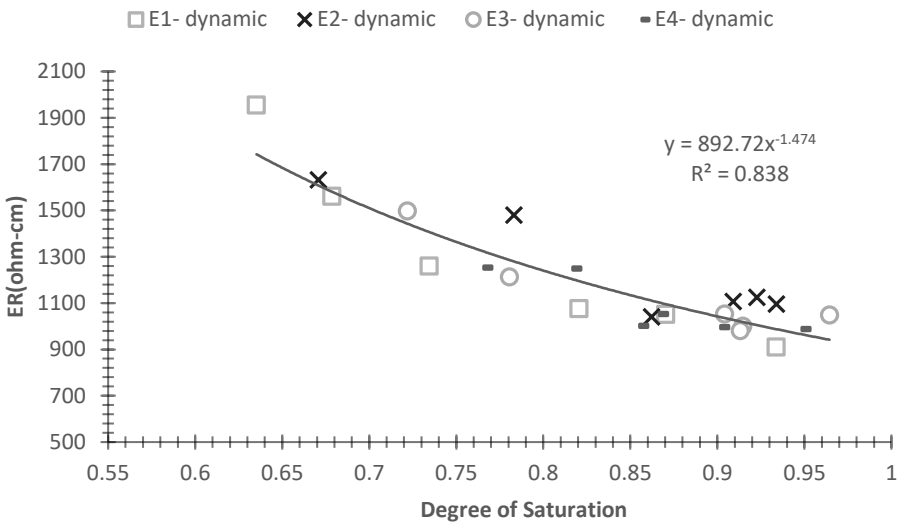

Figure 4.6:The relationship between ER and the degree of saturation of dynamically compacted Terra-rossa soil specimens.

The measurements obtained for static compaction are also observed to be independent of the simulated compaction effort for both soils. Figure 4.7 and Figure 4.8 present the relationship between ER and the degree of saturation under 4 various static compaction efforts for Alluvial clay and Terra-rossa soil respectively.

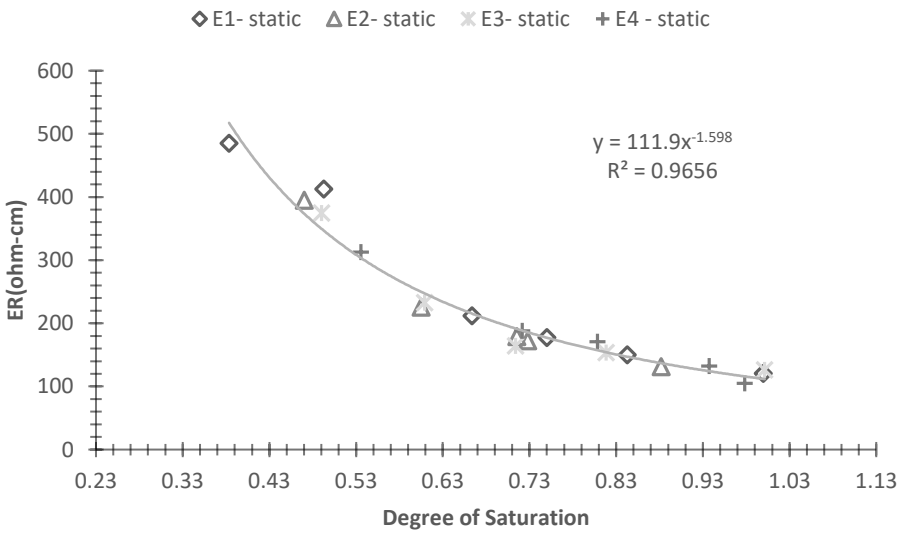

Figure 4.7: The relationship between ER and the degree of saturation of statically compacted Alluvial clay specimens.

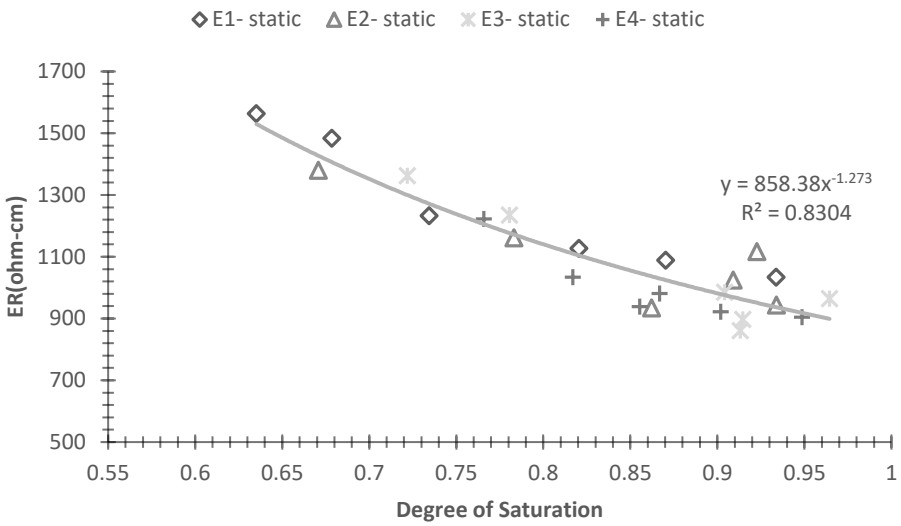

Figure 4.8: The relationship between ER and the degree of saturation of statically compacted Terra-rossa soil specimens.

Dynamically compacted specimens reflected slightly higher ER compared to statically compacted specimens when the specimens have a low degree of saturation ($Sr \leq Sr_{opt}$). However, this variation due to the compaction method diminishes as the specimens approach the fully saturated state. This behavior emphasize that statically prepared specimens have a more oriented fabric compared with the dynamically prepared specimens. The oriented fabric will reduce the path that the current will follows. Figure 4.9 and Figure 4.10 present the relationship between ER and Sr for the statically and dynamically prepared specimens for Alluvial clay and Terra-rossa soil respectively.

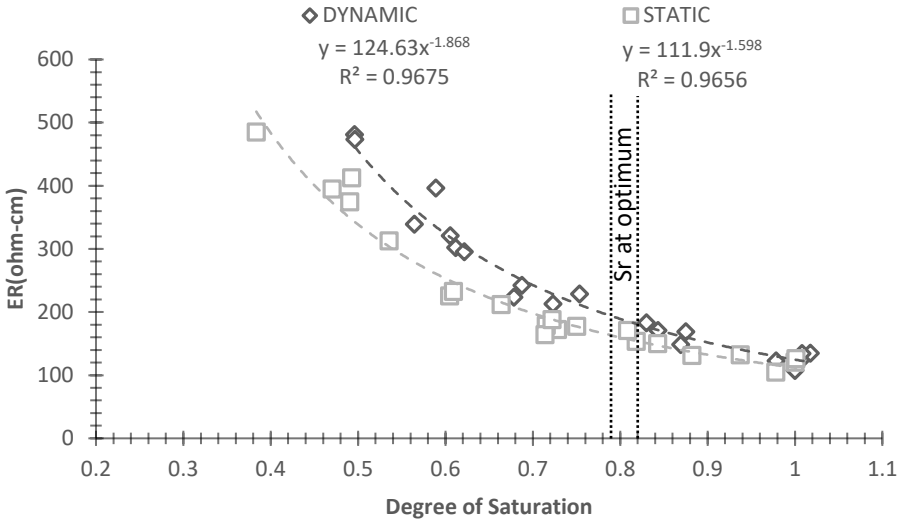

Figure 4.9: The relationship between ER and the degree of saturation of dynamically and statically compacted Alluvial clay specimens.

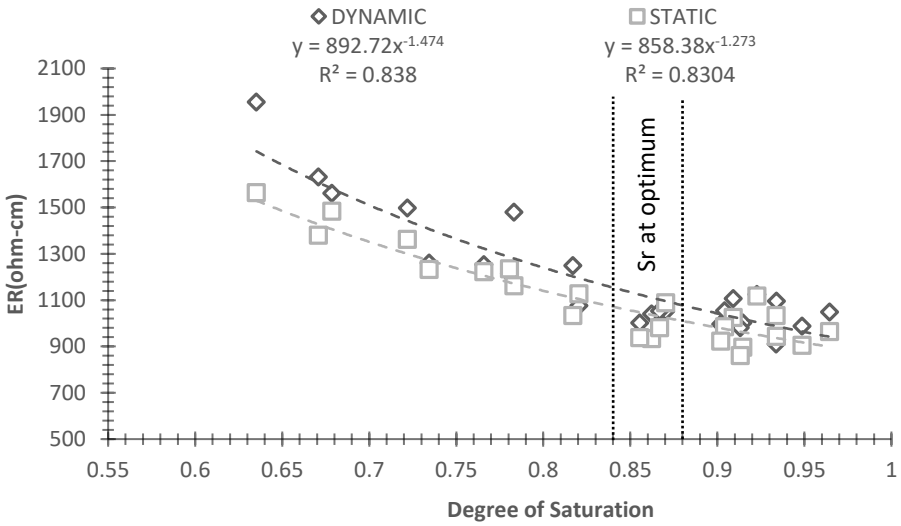

Figure 4.10: The relationship between ER and the degree of saturation of dynamically and statically compacted Terra-rossa soil specimens.

The comparison of results for both soils have shown that there is a significant difference in the ER measured at the fully saturated state. More precisely, the ER of the Terra-rossa soil at fully saturated state is 7.5 times larger than the ER of the Alluvial clay. This can be linked to the fact that Alluvial clay has high concentration of clay size fraction,

4.3.3 Relationship between Electrical Resistivity and Bulk density

It can be concluded with regards to the test results for both soils that the electrical resistivity of the compacted specimen is mainly influenced by the water content and the bulk density of the specimen. As the water content and bulk density increases the ER decreases nonlinearly. Hence, a new relationship is suggested between the electrical resistivity and the multiplication of the bulk density by the water content. This relation shows an independent behavior of the compaction efforts and the method of compaction. Figure 4.11 and Figure 4.12 show the relationship between the electrical resistivity and the multiplication of the bulk density by the molding water content for the statically and dynamically prepared specimens for alluvial clay and Terra-rossa soil respectively.

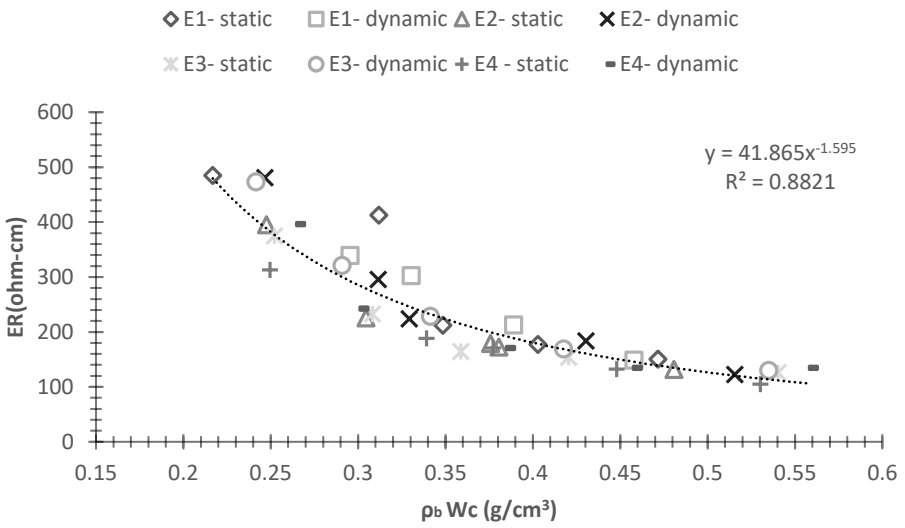

Figure 4.11:The relationship between ER and multiplication of the bulk density by the water content of dynamically and statically compacted Alluvial clay specimens.

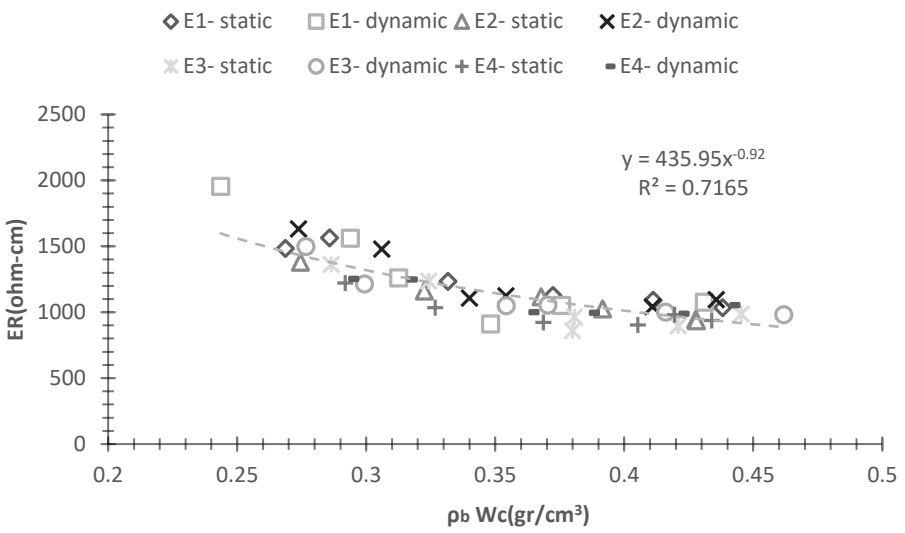

Figure 4.12:The relationship between ER and multiplication of the bulk density by the water content of dynamically and statically compacted Terra-rossa soil specimens.

A three-dimensional plot of the suggested correlation for the Alluvial clay and the Terra-rossa soil are presented in Figure 4.13 and Figure 4.14 respectively.

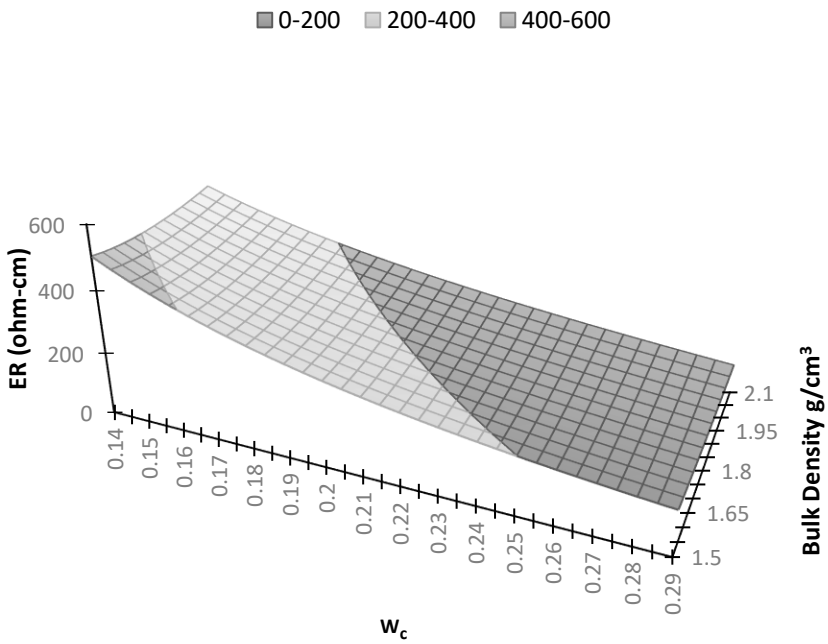

Figure 4.13: 3D plot of the relation between the ER, w_c and bulk density of Alluvial clay specimen.

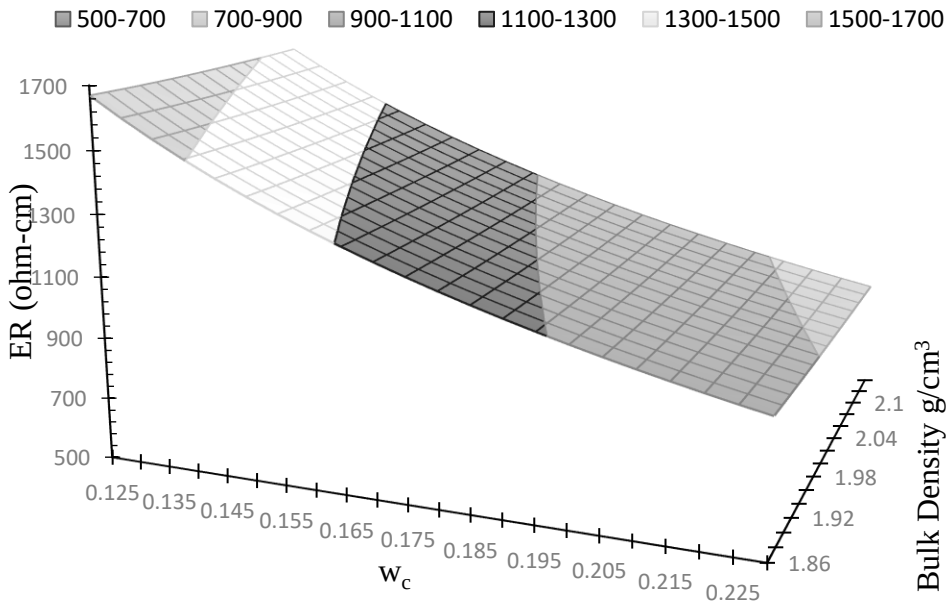

Figure 4.14: 3D plot of the relation between the ER, w_c and the bulk density of the Terra-rossa soil specimens.

4.4 The Undrained Shear Strength

The undrained shear strength of remolded specimens is discussed thoroughly in the literature by various researchers, [11, 12, and 13]. However, the influence of compaction method is not clearly addressed. This section of the study discusses the influence of compaction method on the undrained shear strength of remolded specimens under unconfined compression strength test.

4.4.1 The Undrained Shear Strength in Terms of wc.

The obtained test result of the unconfined compressive strength shows a relationship between the undrained shear strength (cu) and the water content of the dynamically prepared specimens. The relationship exhibited a similar behavior to the compaction characteristic curve. However, the response of the tested soil specimens to the compaction efforts were quite distinctive. Alluvial clay showed higher cu in contrast with higher compaction efforts for the specimen prepared at the dry side of optimum. Ultimately, the undrained shear strength of the Terra-rossa soils was independent of

the compaction efforts. The relation between the cu and the water content of the dynamically compacted specimens for the Alluvial clay and the Terra-rossa soil are presented in Figure 4.15 and 4.16 respectively.

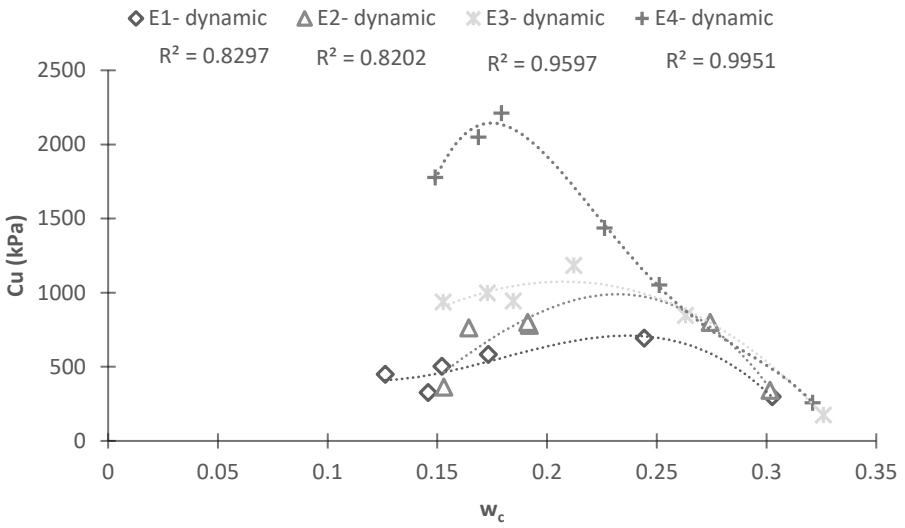

Figure 4.15: The relation between cu and the w_c of dynamically compacted Alluvial clay specimens.

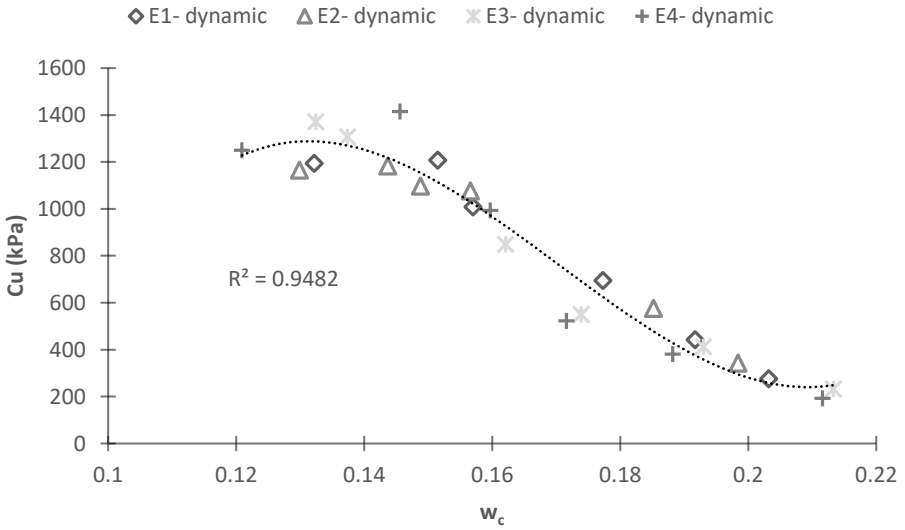

Figure 4.16: The relation between cu and the w_c of dynamically compacted Terra-rossa soil specimens.

The independent behavior of Terra-rossa soil specimens regarding the compaction efforts can be linked to the lack of cohesion among the soil particles where most of the soil body is consisted of coarse-grained soils. On the other hand, the specimens which are prepared using static compaction exhibited a lower undrained shear strength when prepared at the dry side of optimum compared to the dynamically prepared specimens. In addition, the statically prepared specimens of the Terra-rossa soil don't have a definite behavior when plotted against the water content except the ones that prepared using the highest effort (E4). Furthermore, at high water content the undrained shear strength becomes independent of the compaction methods and efforts. The relation between the undrained shear strength with respect to the water content for the statically prepared specimens of Alluvial clay and Terra-rossa soil are presented in Figure 4.17 and 4.18 respectively.

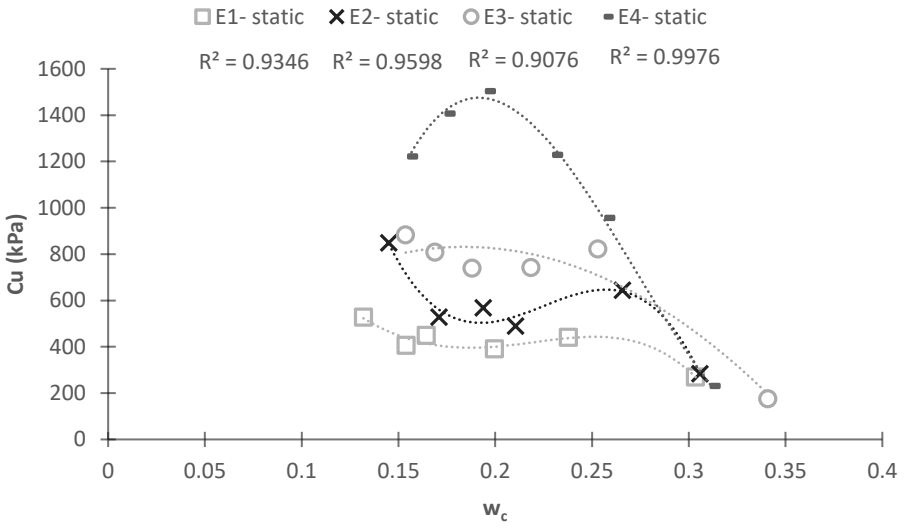

Figure 4.17: The relation between cu and the w_c of statically compacted Alluvial clay specimens.

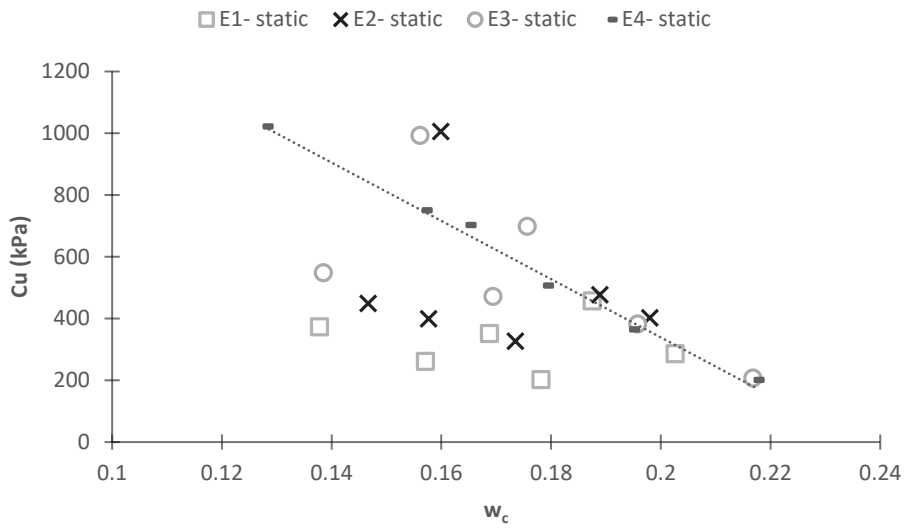

Figure 4.18: The relation between cu and the w_c of statically compacted Terra-rossa soil specimens.

In general, the Alluvial clay has higher undrained shear strength compared to the Terra-rossa soil at a given compaction effort and water content. This is due to the high content of cohesive particles within the body of Alluvial clay unlike the Terra-rossa soil.

4.4.2 Failure Modes Uniaxial Stress

The modes of failure of the specimens that are prepared at dry side of optimum were extremally influenced by the compaction methods. The statically prepared specimens at low water content exhibited a vertical hairline cracks along the direction of shearing and haven't developed failure plane unlike the dynamically compacted specimens. The location of the hairy cracks was always opposite to the direction of the static compaction application point. This suggest that the statically prepared specimens have heterogenous densities along the body of the specimen. Where the part of the specimen near to the point of the compaction application has the highest dry density and the part near the base of the specimen has the least dry density. Figure 4.19 represent a schematic view of the modes of failure at low molding water content.

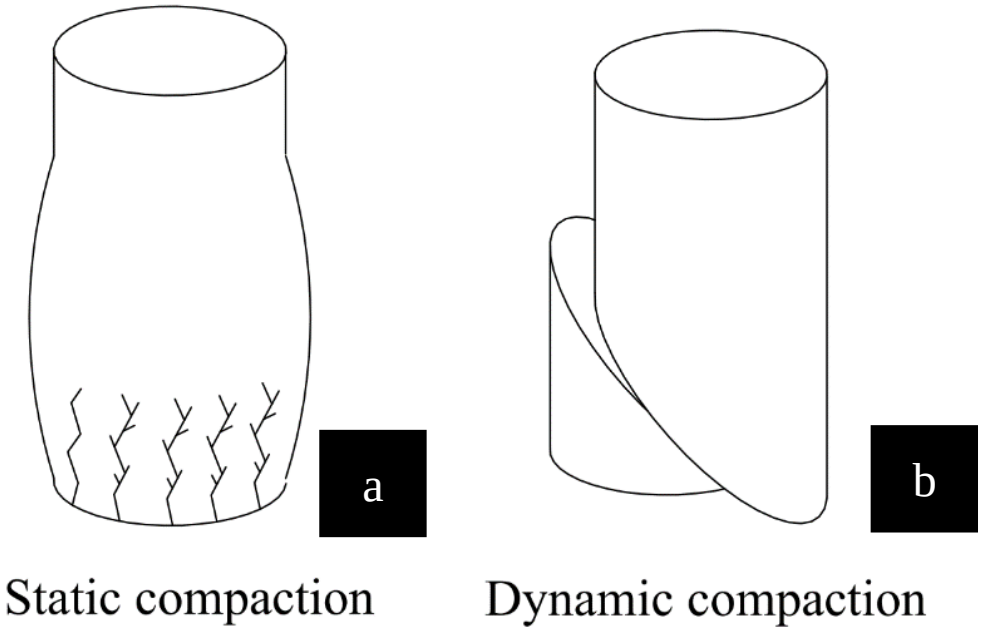

Figure 4.19: (a) The failure mode of the statically compacted specimen at low water content, and **(**b) The failure mode of the dynamically compacted specimen at low water content.

This can be observed as well in the results of the uniaxial compression stress with respect to vertical strain. The statically prepared specimens failed at much lower strains in comparison to dynamically prepared specimens. Figure 4.20 and Figure 4.21 show the relation between the uniaxial compression stress and the vertical strains of the specimen prepared at dry of optimum using both dynamic and static compaction methods for Alluvial clay and Terra-rossa soil respectively.

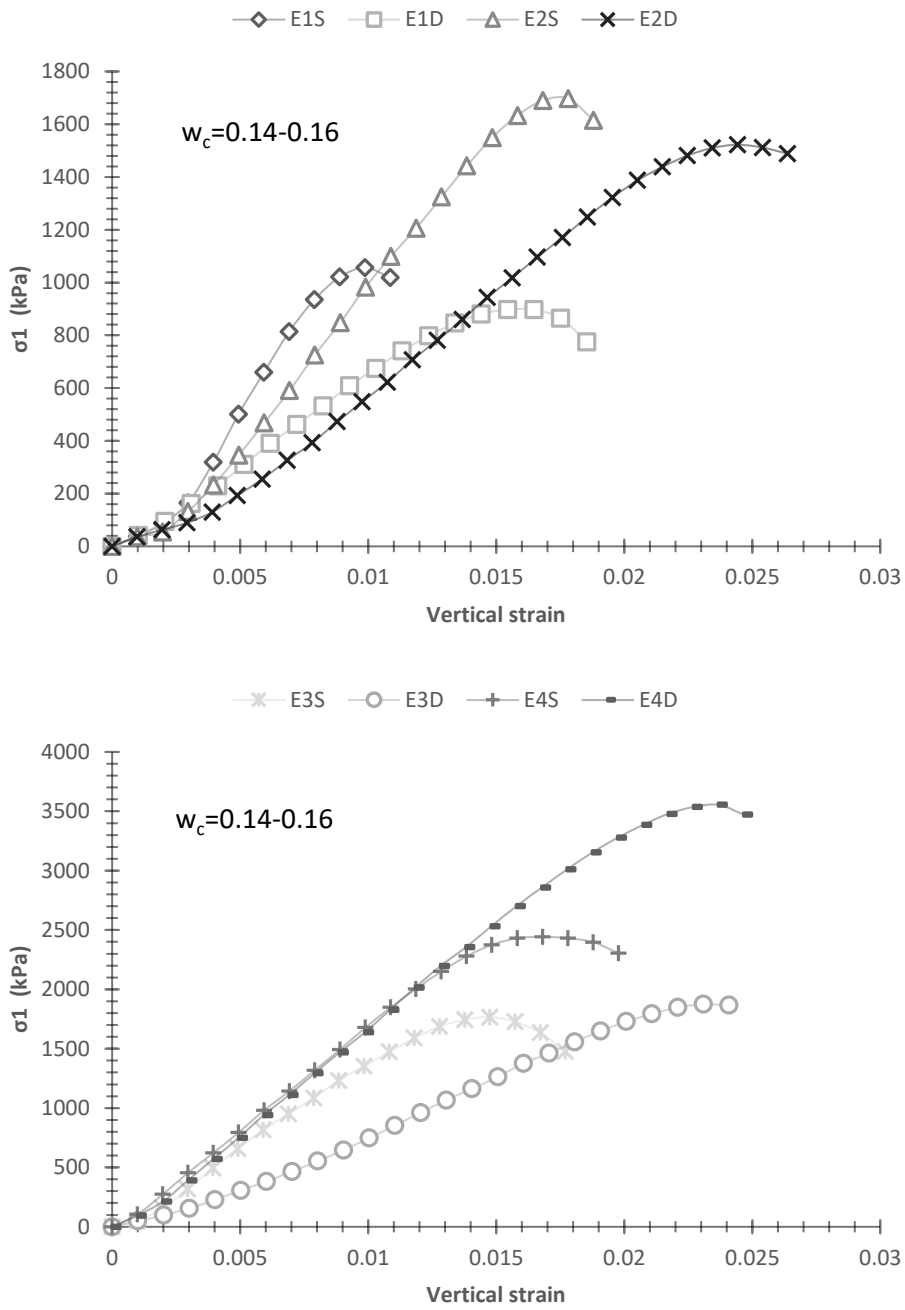

Figure 4.20 : The relation between the uniaxial compression stress and the vertical strain of the dynamically and statically prepared Alluvial clay specimens at low water content.

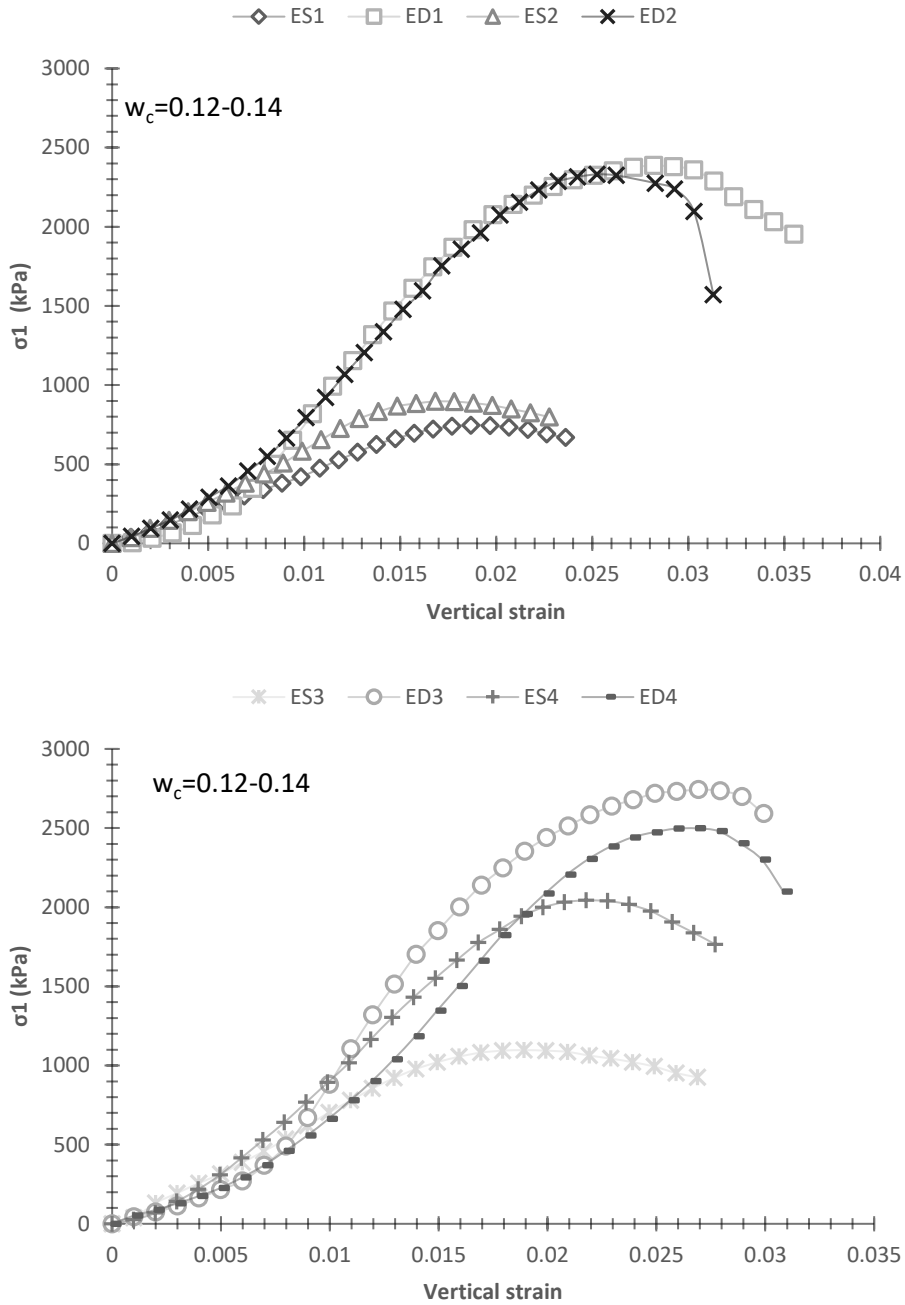

Figure 4.21: The relation between the uniaxial compression stress and the vertical strain of the dynamically and statically prepared Terra-rossa soil specimens at low water content.

4.4.3 The Secant Elastic Modulus (E50) Relations

The specimens prepared using both static and dynamic efforts of the Terra-rossa soil showed a moderate linear regression between the secant elastic modulus and the undrained cohesion. This relation is independent of the compaction methods. As the

secant elastic modulus of the compacted specimens increases the undrained cohesion increases. Figure 4.22 presents the relation between the secant elastic modulus and the undrained cohesion of both statically and dynamically prepared specimens of the Terra-rossa soil.

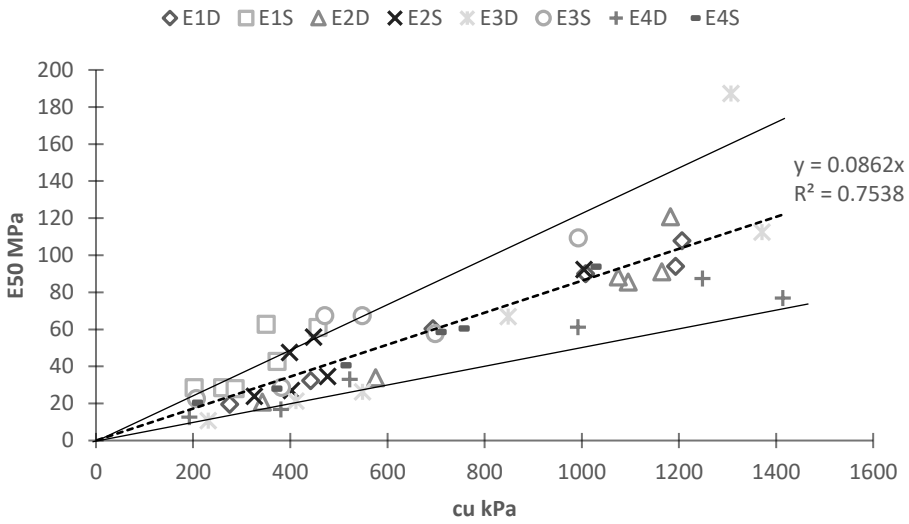

Figure 4.22: The relation between E_{50} and cu of Terra-rossa soil.

On the other hand, the Alluvial compacted clay specimens didn't present independence regarding the compaction methods. In addition, the linear relation between the secant elastic modulus and the undrained shear strength was very poor especially in the case of the statically prepared specimens. Figure 4.23 presents the relation between the secant elastic modulus and the undrained cohesion of both statically and dynamically prepared specimens of the Alluvial clay.

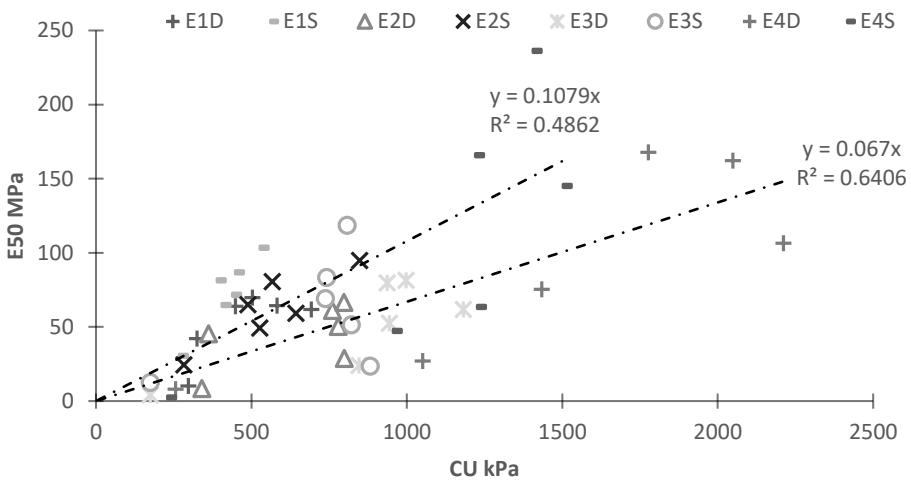

Figure 4.23: The relation between E_{50} and cu of Alluvial clay.

The independence regarding the compaction methods of the test results presented in Figure 4.22 can be linked to the fact that Terra-rossa soil has low plasticity. In other words, the specimens of the Terra-rossa soils don't undergo large deformation before reaching failure. On the other hand, the alluvial clay has high plasticity. Hence, the specimens fail at larger deformation resulting in the variation presented in Figure 4.23 where statically prepared specimens diverge from the dynamically prepared specimens due to the influence of the modes of failure presented in Figure 4.19.

4.5 Compressibility Parameters

The oedometer test results of the compacted specimens show that the initial void ratio is influenced by the compaction effort. Whereas the compaction effort increases the initial void ratio is reduced. Ultimately, the final void ratio was independent regarding the compaction efforts. This behavior is valid for both the cases of the dynamic and static compaction. The relation between the void ratio and the effective stress of the Alluvial clay specimens that are prepared dynamically and statically are presented in Figure 4.24 and Figure 4.25 respectively.

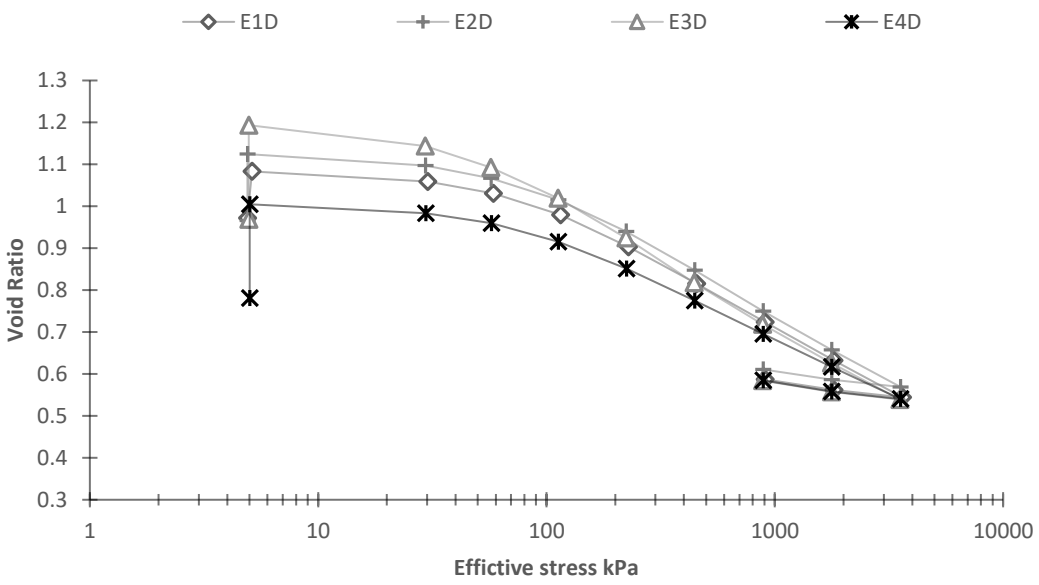

Figure 4.24: The relation between the void ratio and the effective stress of the dynamically compacted Alluvial clay specimens.

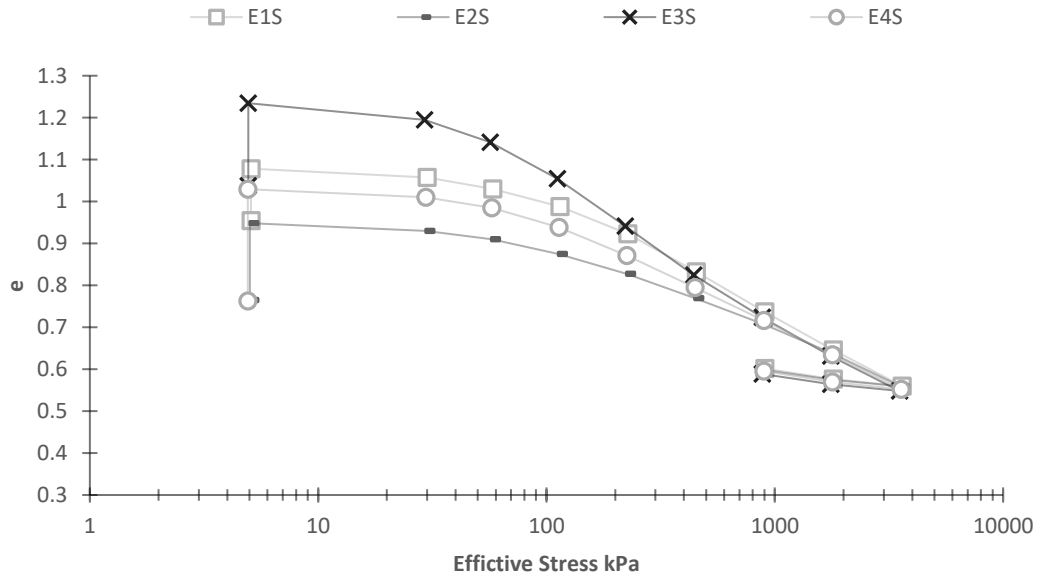

Figure 4.25: The relation between the void ratio and the effective stress of the statically compacted Alluvial clay specimens.

The relation between the void ratio and the effective stress of the Alluvial clay specimens that are prepared dynamically and statically are presented in Figure 4.26 and Figure 4.27 respectively.

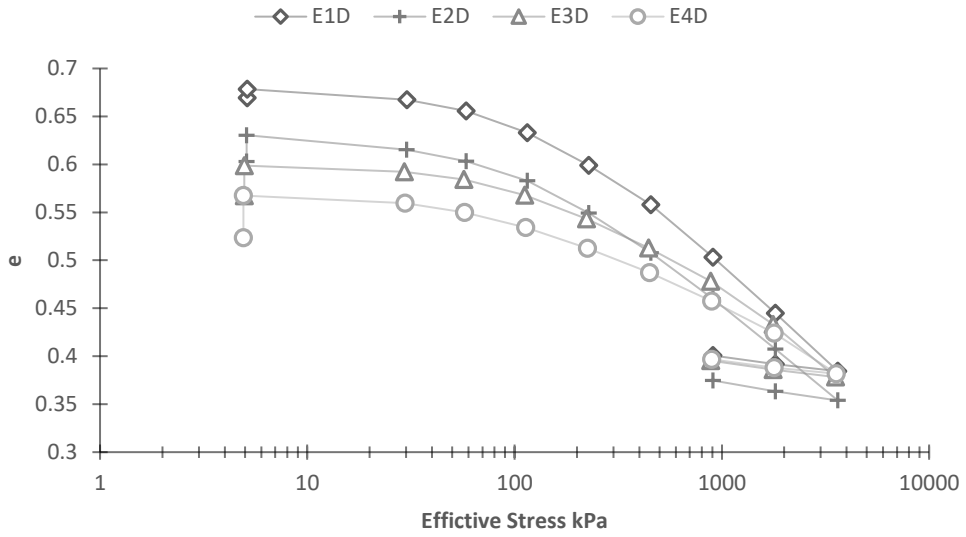

Figure 4.26: The relation between the void ratio and the effective stress of the dynamically compacted Terra-rossa soil specimens.

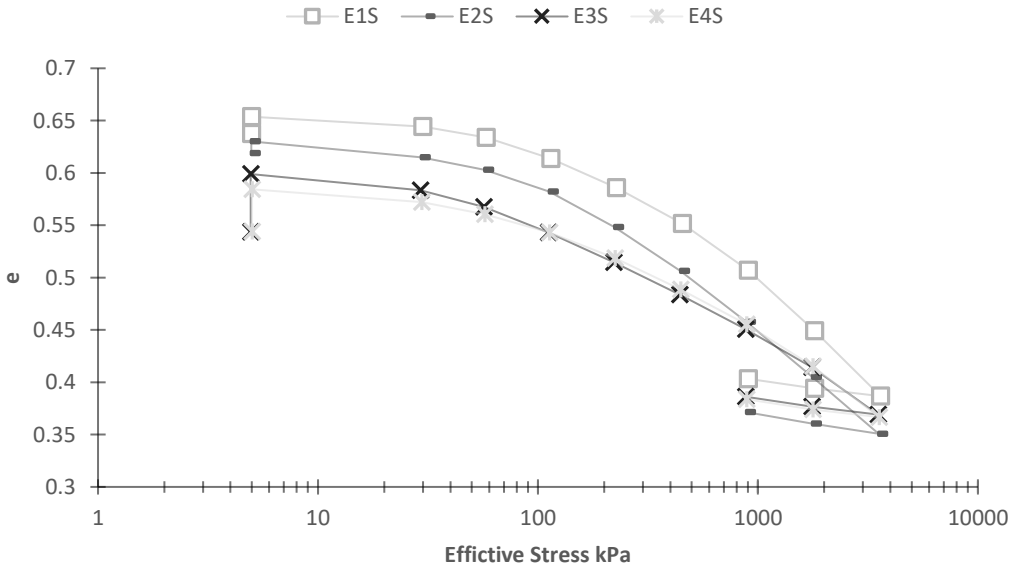

Figure 4.27: The relation between the void ratio and the effective stress of the statically compacted Terra-rossa soil specimens.

It can be seen that all specimens are overlapping at high effective stress except the E2D and E2S of Terra-rossa soil. This can be related to the heterogeneity of the soil. On the other hand, the coefficient of compressibility (Cc) and the coefficient of rebound (Cr) of the Terra-rossa soil show independent behavior regarding the

compaction methods. The values of Cc and Cr of Terra-rossa soil are presented in the Figure 4.28 and Figure 4.29 respectively.

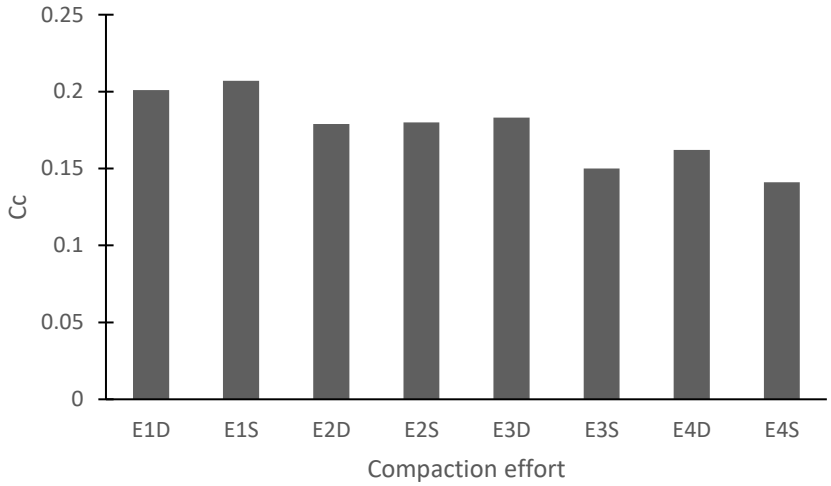

Figure 4.28: The coefficients of compressibility of the Terra-rossa soil.

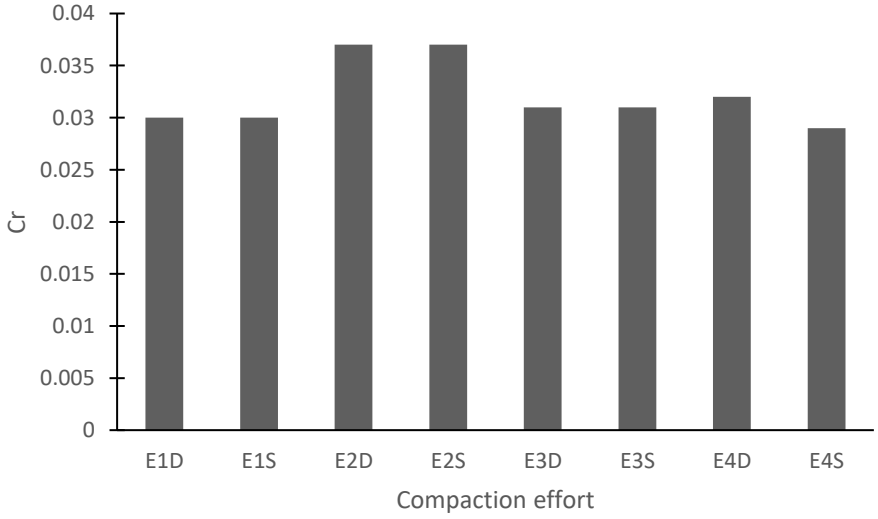

Figure 4.29: The coefficients of rebound of the Terra-rossa soils.

Ultimately, the Alluvial clay shows that the method of compaction is influencing the coefficient of compressibility (Cc) and the coefficient of rebounds (Cr). The values of (Cc) and (Cr) of the Alluvia clay are presented in the Figure 4.30 and Figure 4.31

respectively. Both of the coefficient were higher for the dynamic compaction and lower for the static compaction in most cases.

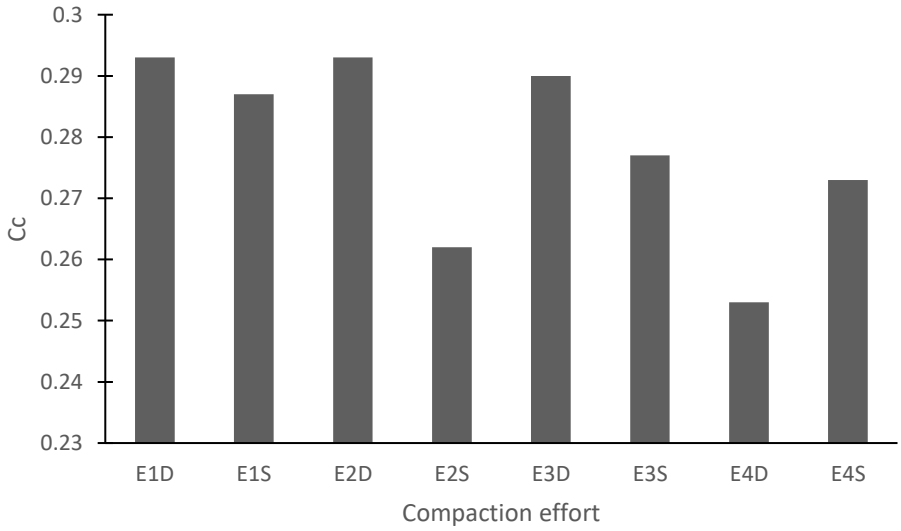

Figure 4.30: The coefficients of compressibility of the Alluvial clay.

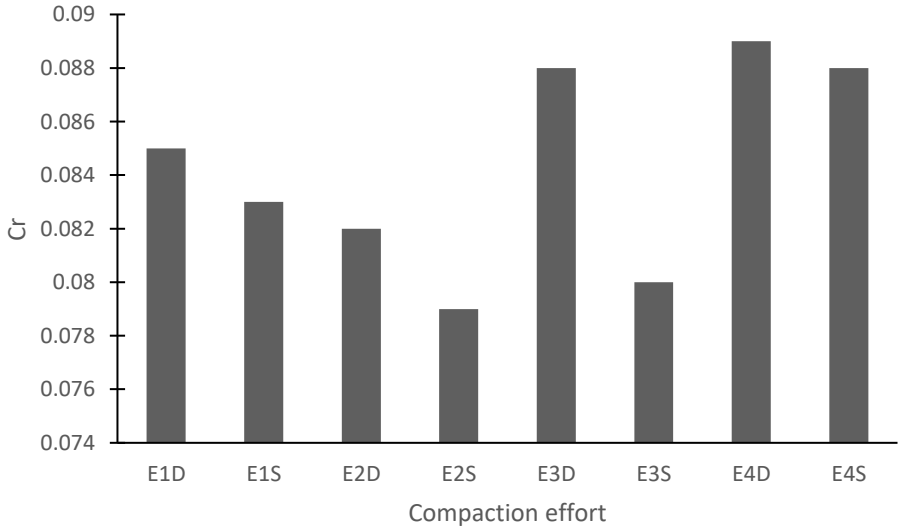

Figure 4.31: The coefficients of rebound of the Alluvial clay.

The determined preconsolidation pressure of the test results exhibited no relation with the compaction effort or the compaction method. Every set of data has its unique

preconsolidation pressure. The results of the preconsolidation pressure of the Alluvial clay and Terra-rossa soil are presented in Table 4.2 and Table 4.3 respectively.

Table 4.2: Preconsolidation pressure of the Alluvial clay specimens

Analysis Method	E1D (kPa)	E1S (kPa)	E2D (kPa)	E2S (kPa)	E3D (kPa)	E3S (kPa)	E4D (kPa)	E4S (kPa)
Maximum curvature [28]	121	147	116	227	72.5	62	126	147.5
Silva [29]	85	106	95	152	50	55.6	93	80
RCL-RVL [30]	79	90	77	109	56.8	50	80	71.5
log-log [31]	152	147	143	233	98	74.2	131.6	150

Table 4.3: Preconsolidation pressure of the Terra-rossa soil specimens

Analysis Method	E1D (kPa)	E1S (kPa)	E2D (kPa)	E2S (kPa)	E3D (kPa)	E3S (kPa)	E4D (kPa)	E4S (kPa)
Maximum curvature [28]	225	342	205	188	356	188	316	421
Silva [29]	186	315	158	143	312	125	262	269
RCL-RVL [30]	150	188	131	126	205	133	133	173
log-log [31]	227	288	219	220	280	220	288	148

There is an inconsistent behavior for the preconsolidation pressure with respect to compaction effort and methods. This can be linked to the fact that the specimens are prepared at different water contents.

4.6 The Swelling Characteristics

The test results of the oedometer testing during the saturation process under 5 kPa show that the statically prepared specimens swell much higher compared to the specimens prepared using dynamic compaction of both soils. The relation between swelling and the time in semilogarithmic scale for the Alluvial clay and the Terra-rossa soil are presented in Figure 4.32 and Figure 4.33 respectively.

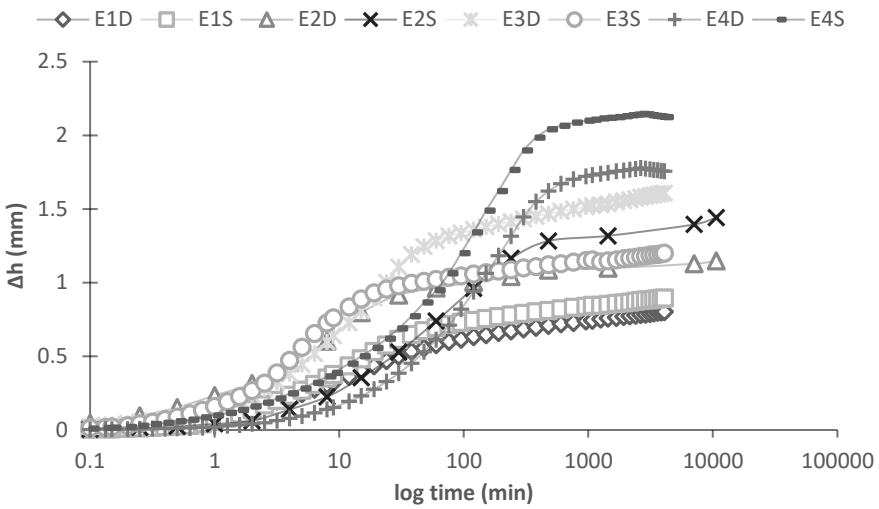

Figure 4.32: The swelling against the log of time of the Alluvial clay.

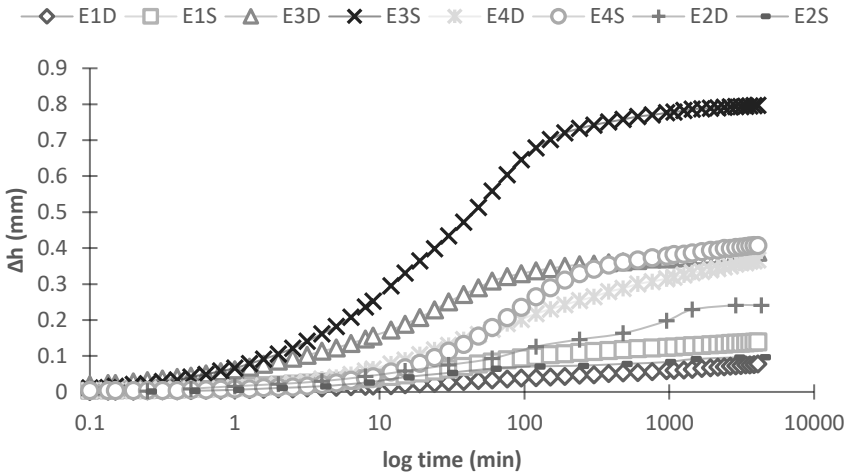

Figure 4.33: The swelling against the log of time of the Terra-rossa soil.

This variation in the swelling potential might be related to the fact that statically prepared specimen has different structure compared with the dynamically prepared specimens. This is can also be observed in the swelling pressure and swelling percentage. In most cases the statically prepared specimens have higher swelling pressure and higher swelling potential. The results of the swelling pressure and the swelling percentage for the Alluvial clay are depicted in Figure 4.34 and Figure 4.35 respectively.

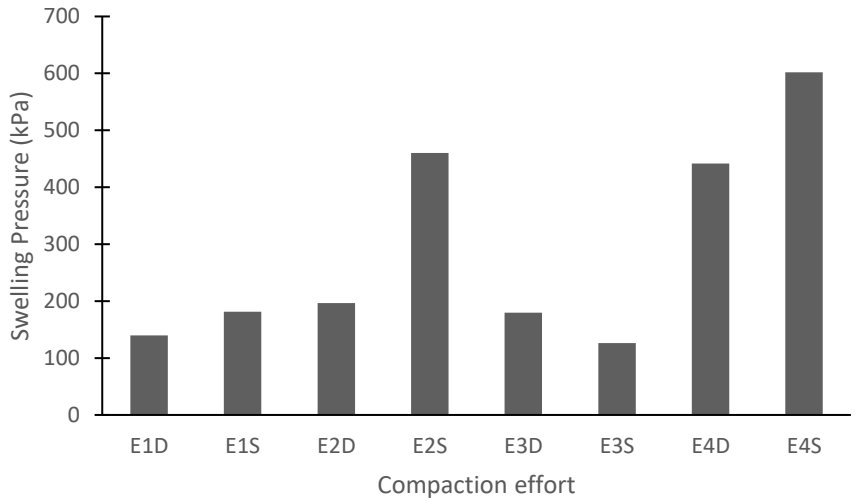

Figure 4.34: The results of the swelling pressure of the Alluvial clay specimens.

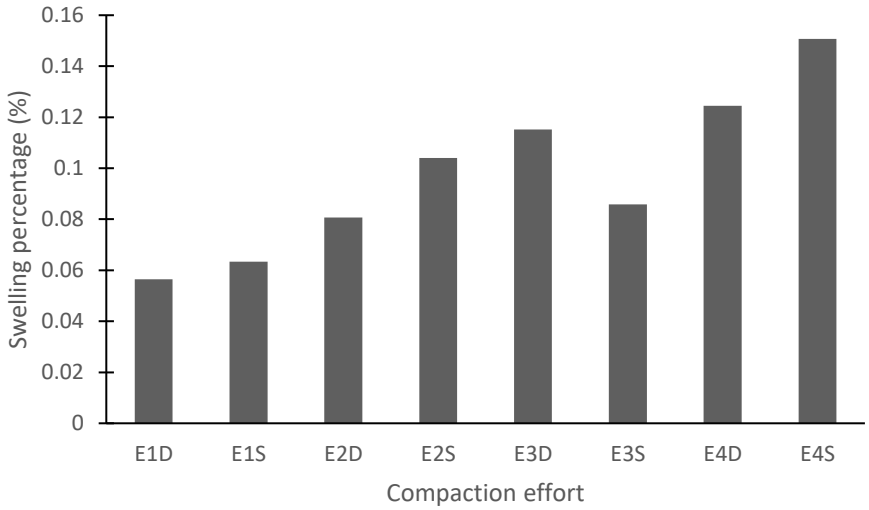

Figure 4.35: The results of the swelling percentages of the Alluvial clay specimens.

The results of the swelling pressure and the swelling percentage for the Terra-rossa soil are presented in Figure 4.36 and Figure 4.37 respectively. Comparing the results of both soils show that Terra-rossa has less swelling potential and less swelling pressure compared with the Alluvial clay. On the other hand, results of tests for both soils show that as the dynamic compaction effort increases both the swelling pressure and the swelling percentage increases. The swelling potential is highly related to the water adsorption potential and hence the initial water contents of the specimens then

have a significant impact on the results. This is clearly seen from the results that, as the initial water content is reduced, which in this testing program also means that the initial density is greater, then the swelling potential is increased as a result.

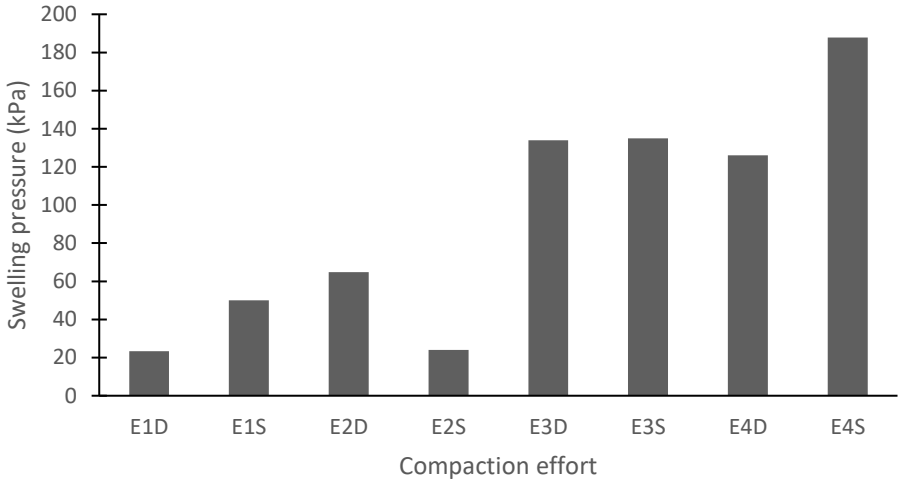

Figure 4.36: The results of the swelling pressure of the Terra-rossa specimens.

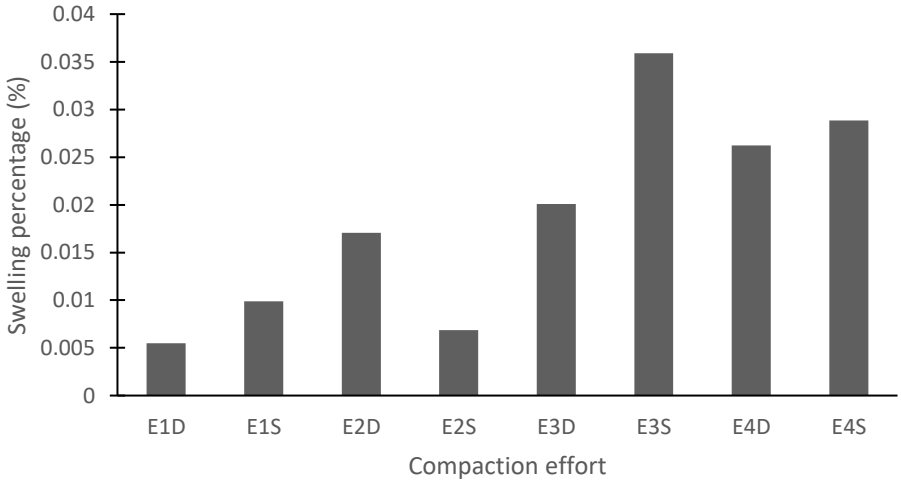

Figure 4.37: The results of the swelling percentage of the Terra-rossa specimens.

Chapter 5

CONCLUSION AND LIMITATIONS

5.1 Conclusion

From the obtained results of the laboratory tests on the influence of compaction methods and effort on the engineering characteristics of two types of cohesive soils, a conclusion can be outlined in the following bullet points;

- The compaction characteristics curve of a given dynamic compaction efforts cannot be represented with a single static stress magnitude. Moreover, the equivalent static stress of a given dynamic compaction effort is a function of the molding water content. As the water content increases the required static stress to achieve a given target density is reduced. On the other hand, the equivalent static stress that represents the optimum values of a certain dynamic compaction effort varies significantly with respect to soil types.

- The ER of compacted specimen is independent of the compaction efforts with respect to degree of saturation. On the other hand, the ER is slightly influenced by the method of compaction when plotted against Sr, where dynamically compacted specimens have higher ER compared with the statically compacted specimens. This emphasize the fact that different methods of compaction may influenced the pore structure of the compacted specimen.

- The undrained shear strength is significantly influenced by the compaction methods. Especially, the specimen that are prepared on the dry side of optimum, statically prepared specimens reflected a significantly lower undrained shear strength. This can be linked to the heterogenous density along the body of the specimen.

- Compressibility charactersistics for the Terra-rossa soil were unaffected by the compaction methods. However, this was not valid for the Alluvial clay where statically prepared specimens showed higher magnitudes for the coefficient of compressibility and rebound index.

- The initial void ratio was highly influenced by the compaction efforts, where higher compaction effort resulted in a lower initial void ratio. On the other hand, the final void ratio was unaffected by the compaction effort where all specimens have almost the same final void ratio.

- The swelling characteristics were significantly influenced by the compaction effort, where the swelling pressure and swelling percentage increase as the compaction effort increases. This can be linked to the fact that as compaction effort increases the optimum water content is reduced. Hence, specimens prepared at high compaction effort will have higher ability to absorb water.

- The swelling characteristics were also influenced by the compaction methods, where in most cases statically prepared specimens showed higher swelling characteristics compared with the dynamically prepared specimens. This can

be related to the fact that statically prepared specimens have more oriented fabric compare to the dynamically prepared specimens.

5.2 Research Limitations

This study investigated the influence of compaction methods on the engineering properties of compacted soils. However, there are many aspects that have not been covered which are listed in the following bullet points.

- Only static and dynamic methods are discussed, where different methods of compaction such as vibratory compaction may result in different behavior.

- The static compaction medium was not fully controlled since water was able to seep out of the mold compaction. Hence confining water movement may exhibit a different behavior.

- Slow rate of static compaction is used where higher rates may not reflect similar behavior.

- The influence of the compaction methods on the soil fabric and structure were not measured.

REFERENCES

[1] A. Zhemchuzhnikov, K. Ghavami and M. dal Toé Casagrande, "Static Compaction of Soils with Varying Clay Content," *Key Engineering Materials*, 2015.

[2] B. M. Das, Principles of foundation engineering, Boston, MA: Cengage Learning, 2019.

[3] J. A. Knappett and R. F. Craig, Craig's Soil Mechanics 8th Ed, London and New York: Spon Press, 2012.

[4] Mitchell, J. K., & Soga, K., Fundamentals of soil behavior, Hoboken, NJ: John Wiley & Sons, 2013.

[5] B. V. Reddy and K. S. Jagadish, "The static compaction of soils," *Ghotechnique*, pp. 337-341, 1995.

[6] C. Hogentogler, Engineering Properties of Soil, New York: McGraw-Hill Book Company, Inc., 1937.

[7] B. Sharma, A. Sridharan, and P. Talukdar, "Static Method to Determine Compaction Characteristics of Fine-Grained Soils," *Geotechnical Testing Journal*, p. pp 1048–1055, 2016.

[8] G. A. Sreelekshmy Pillai and P. P. Vinod, "Re-examination of compaction parameters of fine-grained soils," *Ground Improvement,* pp. 157-166, 2016.

[9] N. S. Pandian, T. S. Nagaraj and M. Manoj, "Re-examination of compaction characteristics of fine-grained soils," *Géotechnique,* pp. 263-366, 1997.

[10] A. Sridharan and H. B. Nagaraj, "Plastic limit and compaction characteristics of finegrained soils," *Ground Improvement,* vol. No.1, no. 9, pp. 17-22, 2005.

[11] M. F. Attom, "The effect of compactive energy properties," *Applied Clay Science,* pp. 61-72, 1997.

[12] John P. Maliziaa, Abdul Shakoorb,, "Effect of water content and density on strength and deformation behavior of clay soil," *Engineering Geology,* pp. 125-131, 2018.

[13] S. J. Wheeler and V. Sivakumar, "Influence of compaction procedure on the mechanical behaviour of an unsaturated compacted clay. Part 2: shearing and constitutive modelling," *Geotechnique,* vol. No. 4, no. 50, p. 369–376, 2000.

[14] Boone M. and Gerken D., "Moisture Content and Relative Compaction Influences on Swell Potential and Strength of a Compacted Residual Soil," in *IFCEE 2015,* San Antonio, Texa, 2015.

[15] Armstrong, C. P., & Zornberg, J. G., "Effect of Fabric on the Swelling Characteristics of Highly Plastic Clays," *PanAm Unsaturated Soils,* 2017.

[16] Tarantino, A. & De Col, E. , "Compaction behaviour of clay," *Géotechnique,* no. 3, pp. 199-213, 2008.

[17] W. Lowrie, Fundamentals of Geophysics, second edition, Zürich: cambridge university press, 2007.

[18] J. Mitchell and K. Soga, Fundamentals of Soil Behavior 3rd Edition, Hoboken, New Jersey: John Wiley & Sons, 2005.

[19] G. Archie, "Electrical-resistivity log as an aid in determining some reservoir characteristics," *Trans. Am Inst. of Min. Engrg,* pp. 146, 318-319, 1942.

[20] Abu-Hassanein, Z. S., Benson, C. H., & Blotz, L. R., "Electrical Resistivity of Compacted Clays," *Journal of Geotechnical Engineering,* pp. 122(5): 397-406, 1996.

[21] Kibria, G. and Hossain, M.S., "Effects of Bentonite Content on Electrical Resistivity of Soils," *Geo-Congress 2014 Technical Papers,* 2014.

[22] C. Atalar, B.M. Das , "Geotechnical properties of Nicosia soils, Cyprus," in *2nd International Conference on New Developments in Soil Mechanics and Geotechnical Engineering, ,* Nicosia, North Cyprus , 2009.

[23] J. Torrent, "Mediterranean soils. In: Hillel, D. (Ed.)," *Encyclopaedia of Soils in the Environment, vol. 2. Elsevier Academic Press, Oxford,* vol. Vol. 2, pp. 418-427, 2005.

[24] Halliday, D., Resnick, R., & Walker, J., Fundamentals of physics: David Halliday, Robert Resnick, Jearl Walker, New York: Wiley, 2003.

[25] Y. Singh, "Electrical Resistivity Measurments: a Review," in *International Journal of Modern Physics*, Bikaner, India, 2013.

[26] Amin Soltani, An Deng, Abbas Taheri, Asuri Sridharan, and A. R. Estabragh, "A Framework for Interpretation of the Compressibility Behavior of Soils," *Geotechnical Testing Journal*, pp. 1-16, 2018.

[27] Zeyad S. Abu-Hassanein, Craig H. Benson, and Lisa R. Blotz, "Electrical Resistivity of Compacted Clays," *Journal of Geotechnical Engineering*, pp. 397-406, MAY 1996.

[28] A. Casagrande, "The Determination of Pre-Consolidation Load and Its Practical," in *First International Conference on Soil Mechanics and Foundation Engineering*, Cambridge, 1936.

[29] F. Pacheco Silva, "A New Graphical Construction for Determination of the Preconsolidation Stress of a Soil Sample," in *Fourth Brazilian Conference on Soil Mechanics and Foundation Engineering*, Rio de Janeiro, Brazil, 1970.

[30] Y. J. a. D. P. Cui, "Yielding and Plastic Behaviour of an Unsaturated Compacted Silt," *Géotechnique,* vol. Vol. 46, no. No. 2, p. pp. 291–311, 1996.

[31] B. T. S. A. a. A. B. M. Jose, "Log–Log Method for Determination of Preconsolidation Pressure," *Geotech. Test. J.,* vol. Vol. 12, no. No. 3, p. pp. 230–237, 1989.

[32] M. Khawlie, "Formation, classification and Land evaluation of soils in Mediterranean areas With special reference to the Southern Lebanon," *Geoderma,* no. 14(2), pp. 172-173, 1975.